Evaluation of the effects of gold nanoparticles (AuNPs) on protein folding in *Escherichia coli*

A thesis presented by

Stanley Makumire

Submitted in fulfilment for the award of the degree of

Master's (MSc) in Biochemistry

Department of Biochemistry and Microbiology, Faculty of Science and Agriculture,

University of Zululand

Supervisor: Prof A. Shonhai

Department of Biochemistry and Microbiology,

University of Zululand

Prof N. Revaprasadu

Department of Chemistry, University of Zululand

Abstract

Gold nanoparticles have shown promising applications, more especially in the biomedical industry. This has seen major improvements in disease diagnostics, therapeutics, imaging and treatment. All this is owed to the unique physicochemical properties possessed by the AuNPs. More studies continue to be carried out on AuNPs as the uses of these nanometer-sized particles are limitless. Water soluble citrate capped gold nanoparticles were synthesized through a slightly modified citrate method. In order to determine size, shape, dispersion and the crystalline nature of the AuNPs, characterization was done using Transmission electron microscopy (TEM) and High resolution transmission electron microscopy (HRTEM). The AuNPs were used to ascertain bacterial-nanoparticle interactions, their effect on *E.coli* growth as well as the effect on the solubility of *E.coli* proteins. The in vitro effects on DNA and protein integrity was also determined. The bacteria work was done by exposing *E.coli* to AuNPs. Imaging was done through TEM and bacterial growth monitored by measuring optical density at hourly intervals. AuNPs were assimilated by the bacterial cells with minimal effects on cellular integrity in $DnaK^-$ cells. DnaK + cells exhibited containment of AuNPs in the cytosol. AuNPs also inhibited *E.coli* growth marginally and had no observable effect on the solubility of *E.coli* proteins at the concentrations tested (25-75 µg/mL) in $DnaK^+$ cells. MDH and MDH in the presence of PfHsp70 were exposed to AuNPs. The AuNPs effect was ascertained by SDS-PAGE. Citrate AuNPs managed to suppress MDH aggregation at low concentrations (2.5-25 µg/mL). At all the concentrations used, the citrate AuNPs complemented the ability of PfHsp70 in suppressing MDH aggregation. The stability of DNA exposed to AuNPs was confirmed by agarose gel electrophoresis and transformations into *E.coli* XL1 blue cells. DNA damage was observed at concentrations (25-100 µg/mL) after exposure for forty-eight (48) hours and for damaged DNA preparations no or fewer colony forming units were observed on agar plates. These findings show that citrate AuNPs are less cytotoxic and

can maintain proteins in soluble form. Although their effect on protein solubility is valuable, citrate AuNPs impact on protein function and are damaging to DNA. Further studies need to be carried out in order to fine tune the physicochemical properties of these particles as a way of improving the biosafety of the AuNPs.

Dedication

I dedicate this study to my wife, Vuyelwa Makumire Jojwana and daughter Ruvarashe Endinaye Makumire.

Declaration

I declare that this dissertation is my own, unaided work. It has been submitted for the degree of Master's in Science at the University of Zululand. It has not been submitted before for any degree or examination at any other University. I also state that all the sources that I have used have been duly acknowledged.

This _____ day of _____ 2014.

Acknowledgement

I wish to thank my Supervisor Prof A. Shonhai, and co-supervisor Prof N. Revaprasadu for all the support, motivation and guidance. Many thanks also to Sixberth Mlowe and Dr. G. Gitau for the remarkable guidance and support. It was a great honor for me to have been chaperoned by you all.

Thank you to all the laboratory mates in Biochemistry and Chemistry, all of whom have been a part of my daily life over the years.

To my parents and friends, for always believing in me and standing by my side throughout the years. I appreciate all you have done for me so my life can be a success.

Above all, I wish to thank the Almighty God for with him nothing is impossible.

Table of contents

List of figures

List of Tables

List of Abbreviations

AuNPs	Gold nanoparticles
PEG	Polyethylene glycol
TEM	Transmission electron microscope
HRTEM	High resolution transmission electron microscope
UV-VIS	Ultraviolet visible
RNA	Ribonucleic acid
DNA	Deoxyribonucleic acid
BSA	Bovine serum albumin
MDH	Malate dehydrogenase
LPS	Lipopolysaccharides
Hsp	Heat shock proteins
PfHsp70	Plasmodium falciparum heat shock protein 70
ATP	Adenosine triphosphate
TiO2	Titanium dioxide
SPR	Surface plasmon resonance
YT	Yeast tryptone
TAE	Tris-acetic EDTA
CFU	Colony forming unit
SDS PAGE	Sodium dodecyl sulphate polyacrylamide gel electrophoresis
PMSF	Phenylmethylsulfonyl fluoride
PEI	Polyethylineimine
TBS	Tris buffered saline
PBS	Phosphate buffered saline
O.D	Optical density
SBD	Substrate binding domain
CAB	Carbonic anhydrase

List of symbols

°C	Degrees celsius
µg	microgram
ng	nano gram
bp	base pairs
nm	nanometers
mL	milliliters
A340	Absorbance at 340 nm
kDa	kilodalton
MW	molecular weight
mM	millimolar
cm	centimeter
g	grams
min	minute
mL	milliliter
OD600	optical density at 600 nm
µg/mL	microgram per milliliter
rpm	revolutions per minute
%	percent
µL	microliter
mg/mL	milligram per milliliter
w/v	weight per volume
v/v	volume per volume
µM	micromolar
V	voltage
a.u	absorbance unit

List of research outputs

Makumire, S., Revaprasadu, N., and Shonhai, A. Concentration dependence effect of citrate capped gold nanoparticles (AuNPs) on the structural integrity of proteins and DNA. Cell Stress Society International Conference (17-22 Aug 2013) Sheffield, United Kingdom. (Oral presentation).

Makumire, S., Revaprasadu, N., and Shonhai, A. Citrate capped gold nanoparticles cause DNA damage and interfere with protein folding in *E.coli*. University of Zululand Postgraduate symposium (3 Nov 2013) Kwadlangezwa, South Africa. (Oral presentation).

Makumire, S., Chakravadhanula, V.S.K., Köllish, G., Redel, E., and Shonhai, A. Immunomodulatory activity of Zinc peroxide (ZnO_2) and Titanium dioxide (TiO_2) nanoparticles and their effects on DNA and protein integrity. (Published in Toxicology Letters, 12 March 2014).

Makumire, S., Revaprasadu, N., and Shonhai, A. Citrate capped gold nanoparticles cause DNA damage and interfere with protein folding in *E.coli*. (Manuscript in preparation).

CHAPTER 1 - Introduction and Literature Review

1.1 Nanotechnology

Nanotechnology is an emerging set of tools, techniques and unique applications involving the structure and composition of materials on a nanoscale (Theis, 2001). The potential of nanomaterials in solving biological problems saw the emergence of bionanotechnology, an intersection of nanotechnology and biology (McQuillan, 2010). In modern years a growth in nanotechnology has been seen, with most emerging applications in drug delivery, imaging and diagnosis (Nel *et al.*, 2006, De Jong and Borm, 2008)with some nanoparticles being used in consumer products such as catalysts, filters, water filtration, semiconductors, cosmetics etc (Nel *et al.*, 2006). Nanotechnology and its applications can potentially improve the quality of life (Chatterjee *et al.*, 2011), although the medicinal benefits and environmental limitations of nanotechnology are only to be realised after an all-encompassing research (McQuillan, 2010). Therefore, it is important to comprehensively understand the reaction, biodistribution, accumulation and excretion kinetics and toxicology of the particles (Lewinski *et al.*, 2008) to ensure safe manufacture and usage of the nanoparticles.

1.2 Nanoparticles

Nanoparticles are by definition, materials at the sub-micrometre scale, usually 1 – 100 nm. According to Hoyt and Masson (2008), the term nanoparticles can only be used in reference to engineered particles and not naturally occurring or by product particles of processes such as welding fumes, fire smoke or carbon black. These particles possess large surface area to volume ratio which makes them highly reactive (Arora *et al.*, 2012). The large surface area and small size of nanoparticles provide properties and applications that are distinct from those of bulk materials

(Fei and Perret, 2009). Generally, a core material and a surface modifier constitute nanoparticles. The surface modifier or capping agent is used to transform the physicochemical properties of the core material (De Jong and Borm, 2008). These rare physicochemical properties can be attributed to small size, chemical composition, surface structure, solubility, shape and aggregation properties (Arora *et al.*, 2012).

1.3 Gold nanoparticles, Synthesis and Applications

1.3.1 Gold nanoparticles

Gold Nanoparticles (AuNPs) are colloidal suspensions of gold particles of nanometre sizes (Pooja *et al.*, 2011). AuNPs in the range 1 – 100 nm exhibit unique optical, electronic and molecular recognition properties hence their use in a variety of applications in bionanotechnology. These properties and applications of AuNPs depend upon their shape. This has seen not only the production of AuNPs of spherical shapes, but other geometries such as rod-shaped nanorods and hollow shells being synthesized (Sonnichsen *et al.*, 2005; Perez-Juste *et al.*, 2005).

1.3.2 Synthesis of gold nanoparticles

The synthesis of AuNPs is based on the reduction of gold salts, such as, chloroauric acid in the presence of a stabilizing agent in aqueous solution as well as in organic solvents (Pooja *et al.*, 2011; Sperling *et al.*, 2008). There are basic methods of synthesis, the first one being the citrate synthesis method which uses trisodium citrate to reduce the gold salt and cap the as formed nanoparticles (Turkevich *et al.*, 1951; Connor *et al.*, 2005). A second commonly used method involves toluene using tetra-octanyl ammonium bromide as a phase transfer reagent (Brust *et al.*, 1994). In order to meet certain research objectives the basic method has been optimised and this has seen a variety of synthesis methods cropping up. (Mandal *et al.*, 2002; Bhattacharya and

Srivastava, 2003; Hung and Leel, 2007). Modifying factors such as temperature and salt concentration results in AuNPs of different shapes and sizes. AuNPs can be functionalized with various organic ligands, such as oligo- or polyethylene glycol (PEG), Bovine serum albumin (BSA), oligo- or polypeptides, oligonucleotides, to create organic-inorganic hybrids with advanced functionality (Ready, 2006). This confers biocompatibility to the nanoparticles and have an influence on the properties of the nanoparticles and hence applications.

1.3.3 Properties of gold nanoparticles and their applications

The easy synthesis and functionalization of gold nanoparticles as well as its less toxic nature and simple detection has made AuNPs become the promising choice in use in various biomedical applications. Applications such as gene and drug delivery, bio imaging, labeling, sensing and cancer treatment, amongst others, are centred on the functional moieties and their capabilities.

Delivery applications take advantage of the inert, non-toxic and biocompatible nature of the gold core (Connor *et al.*, 2005) and also the high surface area to volume ratio provides condensed loading functionalities (Love *et al.*, 2005) incorporating targeting and therapeutic materials. The gold nanoparticle surface structures can easily be modified to incorporate several therapeutic drugs or bio macromolecules (Hermanson, 1996, Sperling *et al.*, 2006). Some AuNPs are able to bind the cell membrane, interact with cell surface lipids, be internalized and easily release their payload in response to stimuli for instance heat, pH and light (Rana *et al.*, 2012).

In labeling and visualization, AuNPs have been used as passive reporters based on the interaction between gold and light (Huang *et al.*, 2007). Gold has been described as an attractive contrast agent that can be visualized with a variety of techniques including phase contrast, dark field microscopy, photoacoustic imaging etc. Molecular recognition properties allow for labeling of

specific molecules or compartments of cells with antibodies to allow for visualisation (Sperling *et al.*, 2008).

The ability of AuNPs to absorb light and mediate heat into their local environment (Govorov *et al.*, 2006) has seen their use as heat sources mainly in anti-cancer therapy (hyperthermia), where an increase in temperature of a few degrees results in cell death. Heat can also be used in the opening of chemical bonds, a concept used in the disassembly of protein aggregates (Kogan *et al.*, 2006). On the other hand, this induced heating can also be used to remotely control the release of cargo molecules from containers such as polymer capsules.

Gold nanoparticles can also be used in active sensor applications. AuNPs exhibit a plasmon resonance around 510 – 530 nm, and the effect of bonded molecules on plasmon coupling can be used for colorimetric detection of analytes and specific biomolecules of significance. When attached to fluorescent material or biomarkers, gold nanoparticles can be used in detection of cancerous cells or tumours. Gold nanoparticle based sensors have a significant impact on diagnostics (Kumar *et al.*, 2007) as their approach is sensitive, rapid and efficient.

1.4 Toxicity of gold nanoparticles

Gold nanoparticles have shown promising usage or applications in various fields of nanobiotechnology and nanomedicine because of their unique properties. This has seen increased administration of these particles into animals and humans (Klebstov and Dykman, 2010). Regardless of their potential, questions are still raised with concerns to the biodistribution and circulation of the AuNPs in the blood stream, their pharmacokinetics and elimination from the organism, and their possible toxicity to the organism as a whole or at the level of cyto- and genotoxicity (Klebstov and Dykman, ibid). This toxicity, like the potential applications, can be

attributed to the physicochemical features, such as surface charge and modifications in addition to shape and size (Freese *et al.*, 2012). Some other studies have also reported toxicity to cells in a time and dose dependent manner. In their study Cho *et al* (2009) reported the accumulation of 13 nm sized PEGylated AuNPs in the liver and induced inflammation and apoptosis in BALB/c mice. Citrate-AuNPs also induced cytotoxicity in human lung AT-II-like cell lines, A549 and NCIH 441(Uboldi *et al.*, 2009). Surface charge has also been shown to have an influence on the uptake properties (Arvizzo *et al.*, 2010) of AuNPs by cells, with cationic nanoparticles having more affinity towards the negatively charged cellular residues (Freese *et al.*, 2012). Increased toxicity due to positively charged AuNPs was seen in Hela (Hauck *et al.*, 2008) and ovarian cancer cells CP70 and A2780 (Arvizzo *et al.*, 2010). On the other hand, cytotoxicity may depend on the type of cell. Patra *et al* (2007) established that 33-nm AuNPs were not toxic to hamster kidney cells (BHK21) or to human hepatocellular carcinoma (HepG2) but were toxic to human carcinoma lung cell line A549. A study of the effects of nanoparticles on cells is of importance for clinical applications.

Cytotoxicity can be a result of various defects brought upon the cell due to the nanoparticle presence such as membrane damage, nuclear or DNA damage, oxidative stress among others. Gold nanoparticles have been implicated in DNA damage and variations in the levels of expression of numerous genes. Balasubramanian *et al* (2010) observed gene expression changes in the liver and spleen of mice after intravenously administering AuNPs. In their work Cho *et al* (2010) reported that 170 genes in BALB/c mice were affected by 4 nm AuNPs and 224 genes induced by 100 nm AuNPs, respectively. Of the genes that showed altered expression, several belong to cellular processes such as apoptosis, cell cycle, inflammation and metabolic processes, stress genes and signal transduction (Cho *et al.*, 2010).

1.5 Interaction of nanoparticles with proteins, DNA and bacterial cells

1.5.1 Effects of nanoparticles on Protein structure and function

Proteins are essential biological entities that are required for proper cellular functioning and the functioning of an organism as a whole. The interaction between nanoparticles and proteins within living organisms is a serious issue that is attracting increasing attention (Fei and Perret, 2009). The secondary structure of proteins can be altered when they bind to planar surfaces whereas the surface curvature of nanoparticles can help proteins maintain their native structure. This might explain how nanoparticles influence protein folding and aggregation. Two factors bring about change to the structure of a protein, namely the inherent properties of the protein and the nanoparticle features. (Fei and Perret, 2009). Smaller nanoparticles have been found to favor native -like protein structure (Vertegel *et al.*, 2004), whereas with larger nanoparticles there is more surface contact between the absorbed proteins and the nanoparticles and this results in stronger interactions between proteins and nanoparticles. This may lead to perturbation of protein structure and favors unfolding or aggregation. On the other hand, the protein coat confers biocompatibility and the ability of nanoparticles to travel within biological fluids as protein-coated units (Lynch *et al.*, 2007). The proteins adsorbed on the nanoparticle surface influence the behavior and destiny of the nanoparticles in nanoparticle-protein interactions.

1.5.2 Nanoparticles on DNA integrity

DNA is a major life constituent as it is a reservoir and transmitter of all genetic material. In eukaryotic cells, DNA is located in the nucleus, mitochondria, chloroplasts, and in prokaryotic cells it is stored in the cytoplasm. Nanoparticles introduced into biological systems can find their way to reach the nucleus by negotiating through cellular barriers. At the nucleus the nanoparticles

can interact directly or indirectly with DNA inducing mutations. Li *et al* (2010) reported that direct or indirect interaction of nanoparticles with DNA results in varying biological and biochemical effects, leading in mutations and genomic instability. Transition metal chromium has been shown to activate molecular oxygen to form species that damage DNA (Casadevall *et al.*, 1999), whereas double stranded DNA was shown to be dissociated by 5 nm AuNPs as a consequence of the strong non-specific interaction between the nitrogenous bases and the gold nanoparticle surface (Yang *et al.*, 2007). Herdt *et al* (2006) also reported that DNA degradation can occur in the presence of a gold surface. These interactions are based on the physico-chemical properties of the nanoparticles, although the structure of the DNA may also contribute to these interactions. This can prompt various defects of cellular function such as cell cycle disruption, cytokinesis arrest and consequently apoptosis.

However, covalent and non-covalent interactions of DNA with some nanoparticles have no effects on DNA integrity. In this way DNA-nanoparticle probes for specific DNA hybridization and recognition of complementary sequences of interest have been developed. It is essential to comprehend these DNA nanoparticle interactions at a cellular or molecular level so as to understand how the particles influence cell functions and how this influence can be controlled for use in therapeutics in nanobiotechnology or nanomedicine.

1.5.3 Interaction of bacterial cells with nanoparticles

Surface features of the cell membrane dominate the initial bacteria-nanoparticle interactions depending critically on size of the nanoparticle and its surface chemistry. The *E.coli* surface is dominated by Lipopolysaccharides (LPS). These are likely to determine the initial physical interaction with nanoparticles (Demento *et al.*, 2009). Another feature of the cell surface is the net

negative charge due to phosphate residues. Cationic nanoparticles might interact with the negatively charged cellular membrane resulting in disruption of the membrane (Goodman *et al.*, 2004).

Different groups of nanoparticles have been shown to act on *E.coli* cells at the nanolevel resulting in biologically undesirable effects. Zinc oxide, iron oxide and silver nanoparticles impact on *E.coli* growth and viability through either membrane disruption and or potential DNA damage. In the bacterial cytosol nanoparticles can interact with vital cell components such as mitochondria, nucleus with adverse effects such as organelle damage, oxidative stress and mutagenesis (Unfried *et al.*, 2007; Allion *et al.*, 2009; Jia *et al.*, 2009; Pan *et al.*, 2009) affecting many cell functions like protein synthesis and metabolism. Under such circumstances, *E.coli* cells respond by expressing a number of molecular chaperones in order to adapt to metabolic changes and survive. Molecular chaperones are proteins that facilitate the folding of other proteins, permitting them to acquire the correct three-dimensional structure necessary for their function (Ellis, 1996). It is highly likely, therefore, that nanoparticles that enter bacterial cells would interact with bacterial proteins, especially members of the molecular chaperone family. Hence the presence of nanoparticles in the cytosol may impact on the protein folding process, most importantly the role of *E.coli* DnaK, a ubiquitous major player in the protein folding pathways of *E.coli*. Some gold nanoparticles have been appraised for their interaction with bacterial cells manifesting minimum cytotoxic effects (Chatterjee *et al.*, 2011). For this reason, the effect of gold nanoparticles on the protein folding machinery of *E.coli* needs to be investigated further. Knowledge from such studies would be crucial to our understanding of the biosafety of gold nanoparticles in light of their application in the nanobiomedical field.

1.6 Role of Molecular Chaperones in Protein Folding

Molecular chaperones are proteins that function to assist the organization of other proteins into their functional native structures (Ellis, 1987). They also prevent and reverse stress induced protein misfolding in the cell (Lindquist and Craig 1988; Morimoto *et al.*, 1994). For this reason, many chaperones, but by no means all, are also stress inducible. Because they were first discovered in drosophila which was subjected to heat stress, the term 'heat shock proteins' (Hsp) was used to first refer to them (Ritosa, 1962). Since proteins tend to aggregate in response to heat stress, it is logical that Hsps are generally upregulated in response to cellular stress. Molecular chaperones consist of several highly conserved families of proteins that are distributed in various cellular compartments (Table 1.1). Hsps are named according to their molecular weights (MW). They range in weight from 8 – 150 kDa and the key subfamilies are the small heat shock proteins (sHsp), Hsp40, Hsp60, Hsp70, Hsp90 and Hsp100. Molecular chaperones are able to differentiate between proteins that are unfolded and those that are folded, as they recognise hydrophobic features of unfolded proteins (reviewed in Boshoff *et al.*, 2004). In cells some molecular chaperones are constitutively expressed and are generally referred to as heat shock cognate (Hsc) proteins, while others are stress induced and designated as Hsp proteins.

Table 1.1 Chaperone families and their mode of action in protein folding

Chaperone	Action	Reference
Hsp 100	ATP driven protein unfolding and disassembly of quaternary polypeptide complexes	Stirling *et al.*, 2003
Hsp 90	Conformational maturation of steroid hormone receptors and signal transducting kinases	Bukau and Horwich, 1998
Hsp 70	ATP dependent folding of nascent peptides	Mayer *et al.*, 2000
Hsp 60	ATP dependent assembly of large multi-protein complexes to the native state	Viitanen, 1990 Bukau and Horwich, 1998
Hsp 40	Bind and stabilise non-native proteins for refolding	Mayer *et al.*, 2000
sHsp	Stabilisation against aggregation during heat shock. Bind and trap denatured proteins	Bukau and Horwich, 1998 Van Monfort *et al.*, 2001

Often cells encounter various stressors, and this leads to protein misfolding and aggregation. During such stressful times some chaperones are over-expressed to protect the cell. The folding is

thought to occur in two steps: a capture step, in which a polypeptide binds to a host molecule to prevent aggregation and a release step, where host molecules release the protein to complete the folding process. In *E.coli* there are two major chaperone systems that act to fold and refold proteins. *E.coli* Hsp70 (DnaK) interacts with co-chaperone Hsp40 (DnaJ) and nucleotide exchange factor Grp E to form the DnaK-DnaJ-Grp E system and chaperonin 60 (GroEL) forms complexes with chaperonin 10 (GroES) to form the GroEL-GroES chaperonin system shown in Figure 1.1.

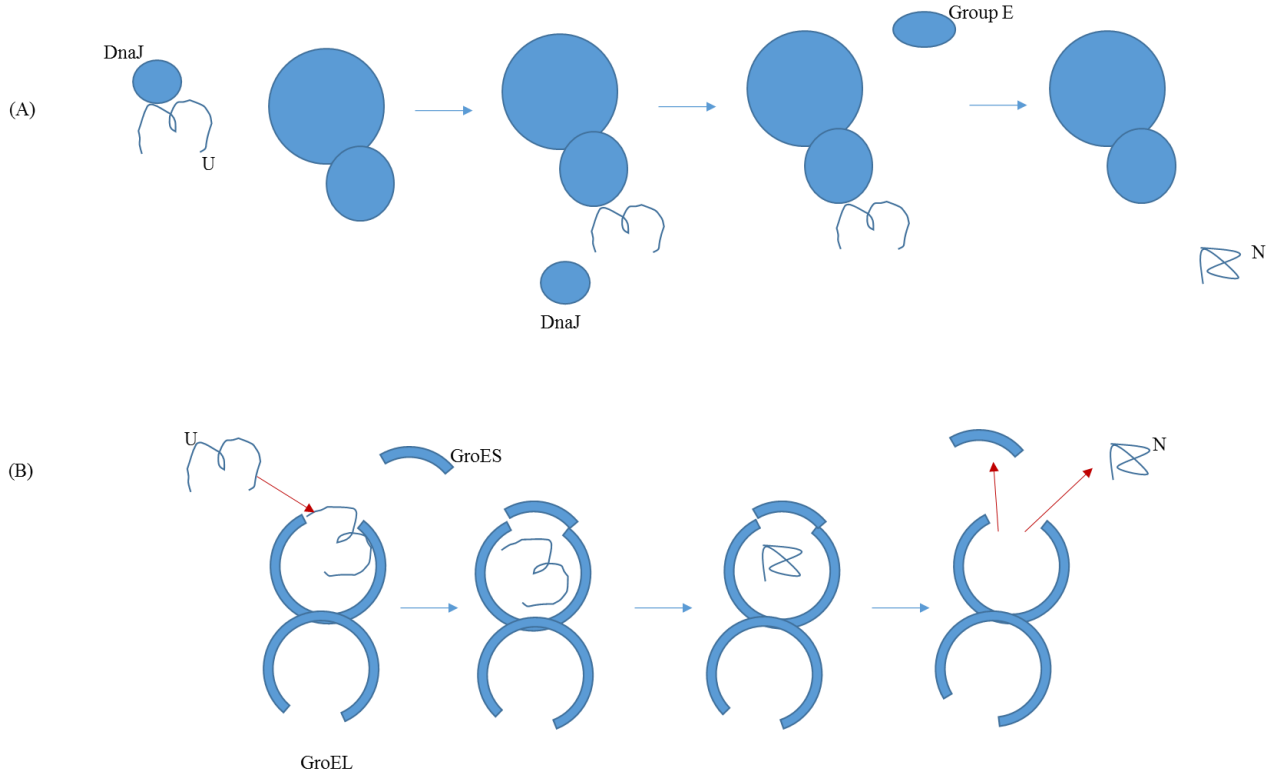

Figure 1.1 Chaperones and protein folding in *E.coli*
(a) DnaK-DnaJ-Grp E chaperone system cooperating to fold an unfolded protein U into its native structure N. (b) The GroEL-GroES chaperone system caging an unfolded protein U, excluding it from the external environment and releasing the protein when completely folded (N).
(Adapted from Protein folding *in vivo*. in *Encyclopedia of Life Sciences*. Nature Publishing Group, London, 2001. Macmillian Magazines Ltd).

Generally native proteins are comprized of an inner hydrophobic core and an outer charged or polar surface. Both the core and the outer layer function to give stability to the tertiary structure of the protein either by hydrophobic or π-stacking interaction or by preferential interaction with the aqueous medium, respectively (Wang *et al.*, 2006).

1.7 The role of *E.coli* DnaK in protein folding

DnaK (*E. coli* Hsp70) is a 69-kDa, monomeric, protein that is comprised of three domains. DnaK is mainly involved in a wide range of functions such as de novo protein folding, host protein refolding, translocation as well as the overall organisation of the adverse effects of stress. As a matter of fact DnaK can be defined as the central organiser of the *E.coli* chaperone network as it is the major bacterial Hsp70 and is the most abundant constitutively expressed and stress inducible chaperone in the *E.coli* cytosol (Bukau and Walker, 1989). Lack of DnaK or disruption of the DnaK gene, leads to protein misfolding and aggregation. This has been shown to be true in studies of three mutant *E.coli* strains devoid of DnaK function, where exposure of these mutants to elevated temperatures caused a loss of cell viability (Table 1.2). The null mutants MC4100Δ*dnaK52::Cm*^{R} *sidB1* and C600 *dnaK103* (Am) *thr::Tn10* grow under a permissible temperature of 30 °C while *dnaK rec A::TcR Pdm1,1* grows normally at 37 °C. The level of synthesis of heat shock proteins was reportedly high in the null mutants, although DnaK was lacking completely. Normal cell growth and cellular division was only realised when a plasmid possessing the DnaK^{+} gene was introduced into these mutants at 42°C (Paek and Walker, 1987), highlighting the importance of DnaK in *E.coli*.

Table 1.2 Characteristics of *E.coli* strains with defective DnaK function

Strain	Characteristic features	Resistance	Reference
BB1553 (MC4100Δ*dnaK52::Cm^R sidB1*)	DnaK gene is disrupted by a cat *cassette* Thermosensitive phenotype Grows normally at 30°C Sensitive to heat and cold Non-permissive temp 40°C	Chloramphenicol	Paek and Walker, 1987.
BB2393 [C600 *dnaK103* (Am) *thr::*Tn10]	Amber mutation on the DnaK gene Non-functional, truncated DnaK Grows normally at 30°C Non-permissive temp 40°C	Tetracycline	Spence *et al.*, 1990; Mayer *et al.*, 2000.
BB2362(*dnaK rec A::Tc^R Pdm1,1*)	Mutant DnaK Grows normally at 37°C Non-permissive temperature is 43.2°C	Tetracycline and Kanamycin	Tilly et al, 1973; Georgopoulos, 1977; Georgopoulos *et al.*, 1979.

Structurally, the DnaK protein is composed of a highly conserved N-terminal ATPase (nucleotide binding) domain, a less conserved substrate binding (SBD) and a C-terminal domain (Chapel *et al.*, 1987; Montgomery *et al.*, 1993; Gragerov *et al.*, 1994). The specific recognition and binding

of unfolded substrates by DnaK is nucleotide dependent. Extended substrates are bound by DnaJ whose role is to deliver them to DnaK-ATP (DnaK bound to ATP). Triggering of the ATPase activity leads to hydrolysis of ATP to ADP giving rise to DnaK-ADP. The ATP state has a low affinity for substrates whereas the ADP Pi state, produced by ATP hydrolysis, shows high affinity for substrates, binding and releasing them slowly giving the substrate time to fold while bound. The co-chaperone Grp E will then stimulate the release of ADP lowering the affinity of substrate by DnaK, thus releasing the substrate. The ATPase activity of Hsp70 proteins is assumed to be fundamental for their biological function (Ang *et al*., 1991; Gething and Sambrook, 1992; Hartl *et al.*, 1992; Craig *et al.*, 1993). Two co-chaperones, Hsp 40 (DnaJ) and nucleotide exchange factor GrpE are responsible for controlling the ATPase activity of DnaK (Mayer 2010; reviewed in Hartl *et al.*, 2011).

1.8 Chaperone-like functions of Nanoparticles

In all cell types, molecular chaperones function to prevent the misfolding and aggregation of proteins. Ideally, the chaperone shields the exposed hydrophobic surfaces revealed by proteins when they unfold. Chaperones bind non-native proteins via hydrophobic or electrostatic interactions (Walter, 2002; Young *et al.*, 2004). Nanoparticle hosts that are hydrophobic in nature can interact with hydrophobic domains of proteins thus preventing aggregation. Highly charged nanoparticles may also interact electrostatically with charged residues on denatured proteins serving as perfect hosts for proper folding (De and Rotello, 2008). Gold nanoparticles are potentially good hosts because of properties such as large surface area and surface turnability (Verma and Rotello, 2005). De and Rotello (2008) demonstrated that negatively charged 2nm core AuNPs functionalized with 2-(10-mercaptodecyl) malonic acid (AuDA) have chaperone-like

properties (Figure 1.2). Electrostatic interactions between negatively charged AuDA with cationic proteins prevented aggregation and assisted the refolding process.

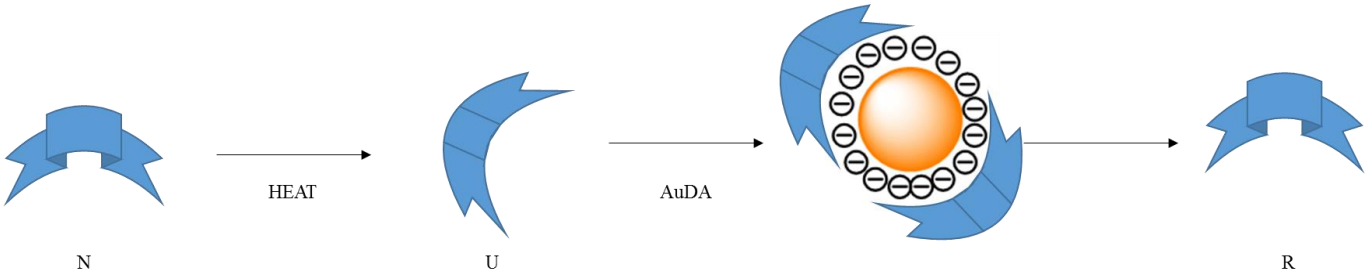

Figure 1.2 Illustration of the thermally induced protein unfolding of native protein (N) and the exposure of the hydrophobic core in unfolded protein (U). This was followed by binding and refolding in the presence of the gold nanoparticle. Release of refolded protein (R) was mediated by addition of sodium chloride (adapted from De and Rotello, 2008).

In yet another study, a nanogel formed by the self-aggregation of pullulan bearing a cholesterol group (CHP), was shown to behave as a molecular chaperone. The nanogel complexed with the heat stressed CAB thus preventing aggregation of the enzyme (Akiyoshi *et al.*, 1999). Recent studies by Luthuli *et al* (2013) confirmed the chaperone-like function of cysteine-AuNPs as they were able to maintain proteins in soluble form during heat stress. Research advances in the activity of these chaperone-like nanoparticles may see their application in improving yields of particular target proteins in heterologous protein production. This can only be understood by investigating the effect of chaperonic AuNPs on protein folding in *E.coli*, a bacteria used as the expression vector in protein biotechnology.

1.9 Hypothesis

Nanoparticles have found a wide range of applications in biological problems, the most important perhaps being in the biomedical field. Be that as it may, the interaction of these nanoparticles with biological materials is not yet fully understood as no simple conclusions have emerged from the variable studies. There is need to further understand these interactions between different types of nanoparticles, cells and biological entities/molecules, with regards to size, shape and surface chemistry of the nanoparticles. This understanding, at a cellular level may be utilized for beneficial biological application.

In cells the primary role of molecular chaperones is to facilitate the folding and refolding of proteins under normal and stressful conditions. As some gold nanoparticles have been demonstrated to possess chaperone-like properties, this could find biological application in the over-production of mammalian proteins in *E.coli* in protein biotechnology. Assimilation by *E.coli* of nanoparticles with such chaperone-like activity might be widely exploited in protein biotechnology to minimise the formation of inclusion bodies and increase the yield of soluble and functionally active proteins. This study hypothesizes that, at the appropriate concentrations citrate coated AuNPs may make *E.coli* proteins more resilient to aggregation as the nanoparticles may bind unfolded proteins through hydrophobic or electrostatic interactions.

However, like most other nanoparticles, even nanoparticles with chaperone properties are likely to be toxic at certain levels of concentrations. In this perspective, these nanoparticles become cell stressors, impacting on the role of molecular chaperones. Understanding how the presence of nanoparticles in the bacterial environment influences bacterial physiology is also important. This

study seeks to also understand this bacterial-nanoparticle interaction in light of protein folding in *E.coli.*

1.10 Objective

The objective of the current study was to investigate whether citrate coated gold nanoparticles assimilated in *E.coli* cells have the ability to promote or inhibit protein aggregation within the bacterial cell under heat stress. Furthermore, the study explored the effects of citrate AuNPs on the function of Hsp70 *in vitro*.

1.10.1 Specific Objectives

1. Synthesis and characterization of citrate coated gold nanoparticles (AuNPs).
2. Monitoring microscopically the interaction of citrate AuNPs and *E.coli* Δ*dnaK 52* cells.
3. Investigation of the ability of AuNPs to promote or inhibit protein aggregation within the bacterial cell under heat stress.
4. Investigation of the effect of AuNPs on the growth rate of *E.coli* BB1553 (MC4100Δ*dnaK52::Cm*^{R} *sidB1*) cells grown in the presence of and absence of AuNPs.
5. Evaluation of the effects of AuNPs on PfHsp70's capability to suppress heat-induced aggregation of MDH *in vitro* (Shonhai *et al*., 2008).
6. Assessment of the effects of AuNPs on the structural integrity of plasmid DNA *in vitro*.

CHAPTER 2

2.0 Methodology

2.1 Synthesis and Characterization of citrate coated gold nanoparticles

The objective of this experiment was to synthesize citrate surface functionalized AuNPs. Ideally, the nanoparticles produced were expected to be small in size (0-20 nm) to ensure access into *E.coli* bacterial cells. A citrate coating was preferred as citrate is readily available, acts as both a reducing and capping agent and the nanoparticles produced would be biocompatible for application.

2.1.1 Synthesis of citrate coated gold nanoparticles

The synthesis of water soluble gold nanoparticles followed the citrate reduction method used by Nghiem *et al* (2010) with slight modifications. Initially 0.3 mM Gold (III) chloride trihydrate ($HAuCl_4.3H_2O$) was reduced by 68 mM and 136 mM sodium citrate tribasic dihydrate ($C_6H_5Na_3O_7.2H_2O$), respectively. The reactions were allowed to proceed for an approximate 10 min. All samples were characterized (section 3.1.2) as AuNPs with varying sizes. Therefore, synthesis of all nanoparticles used in this study followed that 0.3 mM of $HAuCl_4.3H_2O$ was heated to 95 °C with stirring. To this 136 mM sodium citrate tribasic dihydrate ($C_6H_5Na_3O_7.2H_2O$) was added dropwise with continued stirring. Sodium citrate acts as the reducing and capping agent in this case. Upon its addition colour changes in the reaction mixture were noted until a wine red color was observed. The reaction was allowed to proceed for approximately 10 minutes and allowed to cool to room temperature while stirring. Samples were collected and prepared for characterization using Ultraviolet Visible Spectrophotometry (UV-VIS), Transmission Electron Microscopy (TEM) and High Resolution Transmission Electron Microscopy (HRTEM).

2.1.2 Characterization of gold nanoparticles

The UV spectra of these citrate-AuNPs were measured using a Spectroquant Pharo 300. Absorbance for these colloids was measured in the range 200 – 1100 nm in a 1 cm path length cuvette, whereas a JEOL 1010 TEM with an accelerating voltage of 100 kV, Megaview III camera and Soft Imaging Systems iTEM software was used to image the nanoparticles. The images provided information on the morphology, size and dispersion of the AuNPs. To assess the crystal nature of the nanoparticles a JEOL HRTEM with accelerating voltage of 200 kV, Megaview III camera and Soft Imaging Systems iTEM software was used to image the nanoparticles at high magnifications.

2.2 Assessment of the effect of gold nanoparticles on *E.coli* Δ *dnaK 52* cells

Different types of nanoparticles interact differently with bacterial cells, thereby influencing their growth, viability and physiology. It has been reported that biophysical interactions that occur between nanoparticles and bacteria include biosorption, nanoparticle breakdown or aggregation, and cellular uptake, with effects including membrane damage and toxicity (Brayner *et al.*, 2006; Priester *et al.,* 2009). It was interesting to investigate whether citrate AuNPs are internalized by *E.coli dnaK 52* cells, with or without adverse effects on cellular growth and physiology.

2.2.1 Bacterial culture and exposure to gold nanoparticles

All bacterial cultures were performed in double strength Yeast Tryptone (2YT) broth. 2YT was 16 g of Tryptone powder, 10 g of Yeast Extract powder and 5 g of Sodium chloride in 1000 mL of double distilled water. Sterilisation of broth was by autoclaving at 121 °C for 15 min. *E.coli* Δ*dnaK52* were transformed (Section 2.6.4) with either an exogenous DnaK plasmid pQE60/DnaK or with a neat vector plasmid (pQE60) and grown overnight. A volume of 5 µL of *E.coli dnaK 52*

DnaK$^-$ cells from a previously cultured *E.coli* for 14 hours was transferred into 50 mL of fresh 2YT broth. A similar volume of *E.coli dnaK 52* DnaK$^+$ cells (containing exogenous DnaK) was also transferred into 2YT broth. These were incubated aerobically at 30 °C with shaking to optical density (OD_{600}) = 0.6. To each culture, 40 µg/mL of citrate gold nanoparticles were added and incubated overnight. Nothing was added into the *E.coli dnaK 52* control. The cells were grown overnight and pelleted by centrifugation at 14000 rpm and the pellets were washed 5 times with phosphate buffered saline (PBS) (pH 7.5) at 5000 rpm.

2.2.2 TEM analysis of bacterial-nanoparticle interactions

TEM imaging allows for the visualization of interaction that occurs between nanoparticles and bacteria cells in terms of uptake, membrane damage, distribution of nanoparticles within the cells and also any changes in cell size. The pelleted cells were then primarily fixed in 500 µL of buffered 2.5 % Glutaraldehyde for 24 hours. The pellets were washed three times for 5 minutes in phosphate buffer. This was followed by 1 hour post fixing in 0.5 % osmium tetroxide. Washing was done three times for 5 minutes with phosphate buffer. The washed pellets were dehydrated by re-suspending them twice for 5 minutes in 30 %, 50 % and 75 % acetone respectively and twice for 10 minutes in 100 % acetone. The dehydrated samples were infiltrated in 50:50 ratio of epoxy resin (4.1g ERL 4221, 5.9g NSA, 1.43 DER 736 and 0.1g DMAE) and acetone for 4 hours upon which they were left in whole resin for 24 hours. The specimens were polymerised in whole resin for 8 hours at 70 °C in an oven. Thin sections were cut using a microtome. Specimens were mounted on copper grids, stained and viewed on a JEOL 1010 TEM.

2.3 Effect of citrate gold nanoparticles on bacterial growth

2.3.1 Microbial growth monitoring

It is important to understand the effect of NPs on the growth of bacteria as these materials contaminate the environment. Some nanoparticles have been reported to inhibit bacterial growth and others to be nontoxic in the bacterial system (Chartejee *et al.*, 2011, Zhou *et al.*, 2012, Liu *et al.*, 2013). However, different conclusions can be made even for very closely related nanosuspensions. It was interesting to investigate whether the synthesized citrate-AuNPs had any growth inhibitory effect on *E.coli* Δ *dnaK 52*. The *E.coli* Δ *dnaK 52* cells are defiant for DnaK function and exhibit a compromized protein folding pathway. For this reason, they were chosen for use in this study in order to understand the effect of the citrate-coated gold nanoparticles on the protein folding pathway of *E. coli* cells.

Freshly transformed *E.coli* Δ *dnaK 52* cells were inoculated into 2YT broth. This was incubated at 30 °C overnight with shaking. 1 % of culture was transferred into fresh broth in 250 mL flasks. At OD_{600}= 0.6, AuNPs of concentrations 25 µg/mL, 50 µg/mL, 75 µg/mL, 100 µg/mL were added into each flask. The freshly inoculated media with NPs were incubated at 30 °C and 40 °C with shaking at 150 rpm. A duplicate set as the control was run simultaneously made from the same mother culture of the bacteria but without any nanoparticle suspension. The bacterial growth was monitored in samples withdrawn at hourly intervals by recording absorbance at 600 nm. A plot of O.D versus time was made. The method was adopted from Sinha *et al* (2010) with minor adjustments.

2.4 Assessment of the capability of gold nanoparticles to suppress protein aggregation in *E.coli*

2.4.1 Protein solubility studies

Exposure of proteins to high temperatures by heating results in misfolding and subsequently aggregation if the folding pathways fail to operate timeously. *E.coli* cells lacking DnaK are susceptible to heat shock treatment. Subjecting the cells to such a high temperature causes strong protein aggregation comprising approximately 10 % of the amount of pre-existing *E.coli* proteins (Mogk *et al.*, 1999.) The object of the study was to investigate the effect on AuNPs on the solubility state of proteins expressed in *E.coli* under permissible (30 °C) and heat shock conditions (40 °C). An *E.coli dnaK 52* strain was used in this assay. This strain exhibits a thermosensitive phenotype as a result of a disrupted *dnaK* gene (Paek and Walker, 1987). It grows at a normal temperature of 30 °C, but is sensitive to heat and cold (Bukau and Walker 1989, 1990). It was of interest to study the effect of chaperone-like citrate AuNPs on the solubility of *E.coli dnaK 52* proteins under normal and non-permissive temperatures in the presence and absence of DnaK.

Freshly transformed *E.coli dnaK 52* cells were inoculated into 2YT broth and incubated at 30 °C overnight with shaking at 150 rpm. 10 % of culture was transferred into fresh broth in 250 mL flasks. For DnaK expressing cells induction with 0.5 mM isopropyl-1-thio- β-D-galacopyranoside (IPTG) was done at $O.D_{600}$ = 0.6 followed by 1hr incubation. AuNPs of concentrations 25 µg/mL, 50 µg/mL, 75 µg/mL were added into each flask. For the DnaK minus cells, similar AuNPs concentrations were added to each flask at OD_{600}=0.6. Untreated *E.coli* cells were used as the negative control. The flasks were shaken at 150 rpm at 30 °C and 40 °C for 24 hours. The suspension of *E.coli* cells was spun at 3500 rpm for 20 minutes at 4^{o}C and resuspended in 5 ml

lysis buffer (0,01 mM Tris,pH 7.5; 10 mM Imidazole,containing 1 mM (phenylmethylsulfonyl fluoride (PMSF) and 1 mg/ml of lysozyme). The cells were then frozen overnight at -80 ^{o}C. The cells were thawed rapidly and mildly sonicated. The resulting cell lysate was centrifuged at 5000rpm at 4^{o}C for 20 minutes. The supernantant was collected as the soluble fraction and the pellet resuspended in 3 ml of phosphate buffered saline solution (pH 7.5) to constitute the insoluble fraction. Soluble and insoluble fractions were resolved by sodium dodecyl sulphate polyacrylamide gel electrophoresis (SDS-PAGE) at 12% gel density.

2.5 Investigation of the effect of citrate-coated gold nanoparticles on the suppression of heat-induced protein aggregation by Hsp70

2.5.1 Expression and purification of PfHsp70

Hsp70s are highly conserved molecules. As testimony to this, a *Plasmodium falciparum* Hsp70 (PfHsp70) has previously been expressed in *E. coli* cells with compromized Hsp70 function and was able to recover growth of the cells at high temperatures that were otherwise lethal to the cells (Shonhai *et al*., 2005). PfHsp70 is capable of inhibiting the heat-induced aggregation of malate dehydrogenase *in vitro* (Shonhai *et al*., 2008). For this reason, recombinant PfHsp70 was expressed and purified from *E. coli* cells to investigate the effect of gold NPs on its function *in vitro*. A plasmid (pQE30/PfHsp70) which expresses a polyhistidine-tagged form of PfHsp70 was used to transform E. coli XL1 Blue cells as previously described (Shonhai *et al*., 2008). This was followed by the purification of the protein by nickel affinity chromatography as described below.

A colony from freshly transformed *E. coli* XL1 Blue cells was inoculated into 50 mL of 2YT broth and incubated overnight with shaking at 37 °C. This overnight culture was transferred into 450 mL of fresh 2YT broth and incubated to mid exponential growth. 1mM IPTG was used for induction

and hourly samples were collected for the first 5 hours and the cells were harvested at 6 hours. The cell suspension was spun at 5000 rpm for 20 minutes at 4^{o}C and resuspended in 10 ml lysis buffer (0,01 mM Tris,pH 7.5; 10 mM Imidazole,containing 1 mM (phenylmethylsulfonyl fluoride (PMSF) and 1 mg/ml of lysozyme). The cells were then frozen overnight at -80 ^{o}C. The cells were thawed rapidly and mildly sonicated with the addition of 100 µL of 10% polythylenimine (PEI). The resulting cell lysate was centrifuged at 5000 rpm at 4^{o}C for 20 minutes. The supernantant was collected as the soluble fraction and the pellet resuspended in phosphate buffered saline solution (pH 7.5) to constitute the insoluble fraction. The soluble protein extract was mixed with an equal volume of lysis buffer and added into a tube with Ni-NTA resin. These were mixed on a shaking platform for 30 mins. Purification of the protein followed the Ni-NTA procedure for purification of His-Tagged proteins by Batch method (Appendix B2). The eluted protein was directly analysed by SDS PAGE and confirmed by Western Blotting using anti-PfHsp 70 antibodies. The protein was then poured into a dialysis tubing and the tube immersed in dialysis buffer (60.4 g Tris, 87.6 g NaCl, 3.4 g Imidazole, 500 mL Glycerol mixed and pH adjusted to 7.5). Dialysis of the protein was performed at 4 °C for 24hrs. The buffer was changed after every 4 hours with an overnight incubation. The protein was finally concentrated by covering the tubing with polyethyleneglycol (PEG). A Bradford assay was conducted to determine the concentration of the portein.

2.5.2 Effect of citrate-coated gold nanoparticles on the protein aggregation inhibition function of PfHsp70

MDH is a well-known aggregation prone protein. Its heat-induced aggregation is suppressed by Hsp70 *in vitro* (Shonhai *et al.*, 2008). Recently, Luthuli *et al* (2013) showed that cysteine capped AuNPs could maintain certain proteins in soluble state under heat stress. This study sought to assess the effects of citrate-AuNPs on the stability of MDH under heat stress. Also of interest was the nanoparticle effect on PfHsp 70 activity *in vitro* given the tendency of cysteine AuNPs to interact with proteins bovine serum albumin (BSA) and human Hsp70 (hHsp70) (Luthuli *et al.*, 2013).

Different volumes of assay buffer (20 mM tris, pH 7.4; 100 mM NaCl; (Shonhai *et al.*, 2008) were placed into eppendorf tubes. Varying concentration of AuNPs ranging between 2.5 and 100 µg/mL were added into respective tubes. Into the separate tubes the respective proteins were added to a final concentration of 1.3 µM for PfHsp70 and 0.65 µM for MDH (Sigma Aldrich, St. Louis, MO). Tubes containing MDH alone and MDH in the presence of PfHsp70 were used as negative and positive controls respectively. The solutions were mixed thoroughly and 300 µL of each solution was placed in wells in triplicate on a 96 well plate. The plate was placed in a Biotech ELX 800 Plate Reader at 48 $^{\circ}$C and absorbance was measured at 340 nm. Note that protein aggregation was monitored based on the development of turbidity. Readings were taken every 5 minutes for 60 min.

2.5.3 Assessment of the effect of citrate gold nanoparticles on the solubility of heat stressed MDH

In a reaction, 20 µl samples containing 1 µM MDH were pre-incubated in the presence of AuNPs at a final concentration of 25, 50, 75 and 100 µg/mL and also in the additional presence of PfHsp 70. An additional tube containing MDH alone was included as negative control. The reaction mixtures were incubated at 48°C for 20 min. Soluble protein was separated from aggregated protein by centrifuging the samples at 14 000 rpm for 10 min. A total of 15 µl of the supernatant was removed (soluble protein) and mixed with 5 µL SDS-PAGE loading buffer. The remaining pellet was re-suspended in SDS-PAGE loading buffer. The samples were boiled briefly and analysed by SDS-PAGE, a 12% gel run at 120V for 1 hour. The gel was stained with Coomasie stain.

2.6 Assessment of the effect of gold nanoparticles on DNA integrity

The introduction of nanoparticles into cells has been shown to be of potential interest in gene and drug delivery. However, it is important to ascertain the risks associated with interaction of nanoparticles with DNA. Investigating the effect of citrate-AuNPs on the structural integrity of plasmid DNA was key in addressing genotoxicity concerns.

2.6.1 Purification and Quantification of plasmid DNA

E.coli XL1 Blue cells transformed with plasmid pQE60/DnaK were cultured in 5 mL 2YT broth overnight at 37 °C on a shaker. The cultures were centrifuged at 14500 rpm for 1 min and the resultant pellet was used for DNA purification following the ZymoResearch Plasmid miniprep™ kit-(Classic) protocol (Appendix B6).

Into a 1mL quartz cuvette 10 µl of plasmid DNA was mixed with 990 µl of distilled water to a dilution factor 1:100. This was placed in a Cecil CE 2021 2000 series spectrophotometer and absorbance measured at 260 nm. DNA quantity was calculated using formula:

Concentration (µg/ml) = (**A260** reading) × dilution factor × 50µg/ml.

2.6.2 Confirmation of the integrity using restriction analysis

The integrity of the pQE60/DnaK plasmid DNA was confirmed by restriction analysis using the enzyme FastDigest *Nco* I (Thermoscientific, Illinois, U.S.A). This enzyme cuts the plasmid twice at 114 and 1323 base pairs, respectively. Two test tubes were set up, tube 1 containing an aliquot of DNA that was not treated with restriction enzymes and tube 2 was treated with 1 µl of restriction digest enzyme *Nco* I. Both tubes were incubated at 37°C for approximately 15 min. To stop the reaction 5 µl of gel of DNA loading dye was added and samples were analyzed by agarose gel electrophoresis.

2.6.3 Assessment of the effect of citrate-gold nanoparticles on the integrity of plasmid DNA.

Plasmid pQE60/DnaK was extracted, quantified and confirmed through restriction digestion. The plasmid was exposed to varying concentrations (25–100 µg/mL) of citrate-capped gold nanoparticles as per method by Dunpall *et al* (2012) with modifications. Untreated plasmid DNA was used as a negative control and pQE60/DnaK mixed with 1000 µM titanium dioxide as positive control. The resultant mix was incubated at 37ºC for 48 hours. After 24 hours 15 µL of each sample was withdrawn and mixed with 5 µL of DNA loading dye and analysed by agarose gel electrophoresis. The remaining sample was incubated for a further 24 hours, upon which each was run on agarose gel. For agarose gel analysis, samples were loaded on a 1.0 % agarose gel and run at 100 V for 60 minutes.

2.6.4 Confirmation of plasmid DNA damage using transformed *E.coli* XL1 blue cells

Plating of bacteria was done on 2YT agar plates. 2YT agar plates contained 16 g of Tryptone powder, 10 g of Yeast Extract powder, 5 g of Sodium chloride and 9.0g of Agar bacteriology in 1000 mL of double distilled water. Autoclaving was done at 121 °C for 15 min to ensure sterility and this was supplemented with 100 µg/mL ampicillin before pouring under sterile conditions

In order to further confirm the effect of the nanoparticles on the integrity of plasmid DNA, bacterial transformations were conducted using DNA that had been exposed to various concentrations of citrate-AuNPs. The pQE60/DnaK plasmid possesses ampicillin resistance and, therefore, bacterial cells transformed using this plasmid were expected to grow in the presence of ampicillin. 5 µL of the various nanoparticle treated DNA samples was mixed with 100 µL of *E.coli* XL1 Blue cells. These were left to stand on ice for 30 minutes followed by heat shock treatment (42 °C) on a heating block for 45 seconds. The samples were replaced on ice for 10 minutes after which 900 µL of 2YT broth was added into each tube. Incubation was done at 37 °C for 1 hour. When the incubation time elapsed, 100 µL of each sample was spread in doublet on YT-agar plates. These were incubated overnight at 37 °C. Following the overnight incubation the numbers of colony forming units in each plate were determined.

CHAPTER 3 - Results

3.1.1 Synthesis of citrate capped gold nanoparticles

The synthesis of gold nanoparticles followed the citrate reduction method originally coined by Turkevich *et al.*, 1951 with slight modification as per method by Ngiem *et al* (2010). The nanoparticle suspensions obtained were stable at room temperature and in water. This colloidal stability was as a result of the citrate coating since citrate which acted as a reducing agent was also the capping agent. In the presence of the capping agent, the nanoparticles possessed a net negative charge as the citrate ions produced a negative charge on the nanoparticle surface (Zhou *et al*., 2012). The AuNPs suspensions possessed the characteristic wine red color (insert Figure 3.1) and this was confirmed by UV-VIS spectroscopy. Initially, 0.3 mM $HAuCl_4.3H_2O$ was reduced with 68 mM and 136mM $C_6H_5Na_3O_7.2H_2O$. The absorption spectra for the nanoparticles exhibited peaks at 519 nm and 523 nm (Figure 3.1), which fall within the distinct absorption peak from the surface plasmon absorption of gold nanoparticles which ranges between 510 - 530 nm (Sobczak-Kupiec *et al.*, 2011). The absorption spectra for AuNPs from a 68 mM citrate reduction was slightly broad as compared to that from a 136 mM citrate reduction. The differences in the broadness of the absorption spectra could suggest differences in the size of the particles from the 2 citrate reductions. The concentration of citrate is known to limit the growth of nanoparticles (Doyen *et al.*, 2013) and hence the higher citrate concentration used (136 mM) could have resulted in smaller nanoparticles as characterized by the narrower absorption spectra. Since the reaction time was fairly low, approximately 10 min, the reduction process under these conditions was high.

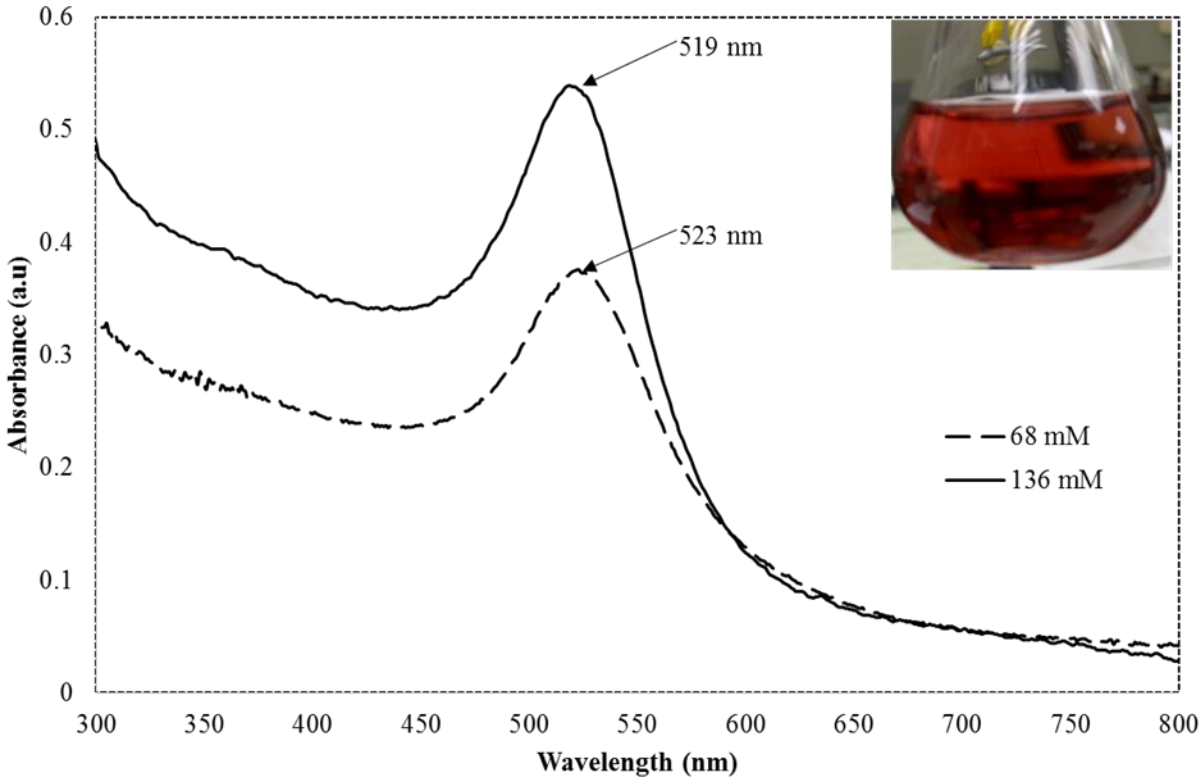

Figure 3.1: The absorption spectra of citrate capped AuNPs.
0.3 mM gold salt was reduced with 68 mM and 136 mM tri-sodium citrate. The insert shows the red wine suspensions obtained.

3.1.2 Assessment of particle morphology by Transmission Electron Microscopy (TEM) and High Resolution Transmission Electron Microscopy (HRTEM)

In nanoparticle synthesis, the reaction conditions influence nanoparticle characteristics such as shape and size. For the synthesized citrate AuNPs, size and shape were determined by TEM. To obtain TEM images, the AuNPs were centrifuged, re-suspended in double distilled water and sonicated. Approximately 2 µL of the suspensions was placed on a copper grid, dried and imaged. Spherical and monodisperse nanoparticles were observed (Figure 3.2). The average diameters were obtained to be 26.7 nm (Figure 3.2A) and 16.2 nm (Figure 3.2 B) with standard deviations of ± 3.14 nm and ± 2.59 nm respectively.

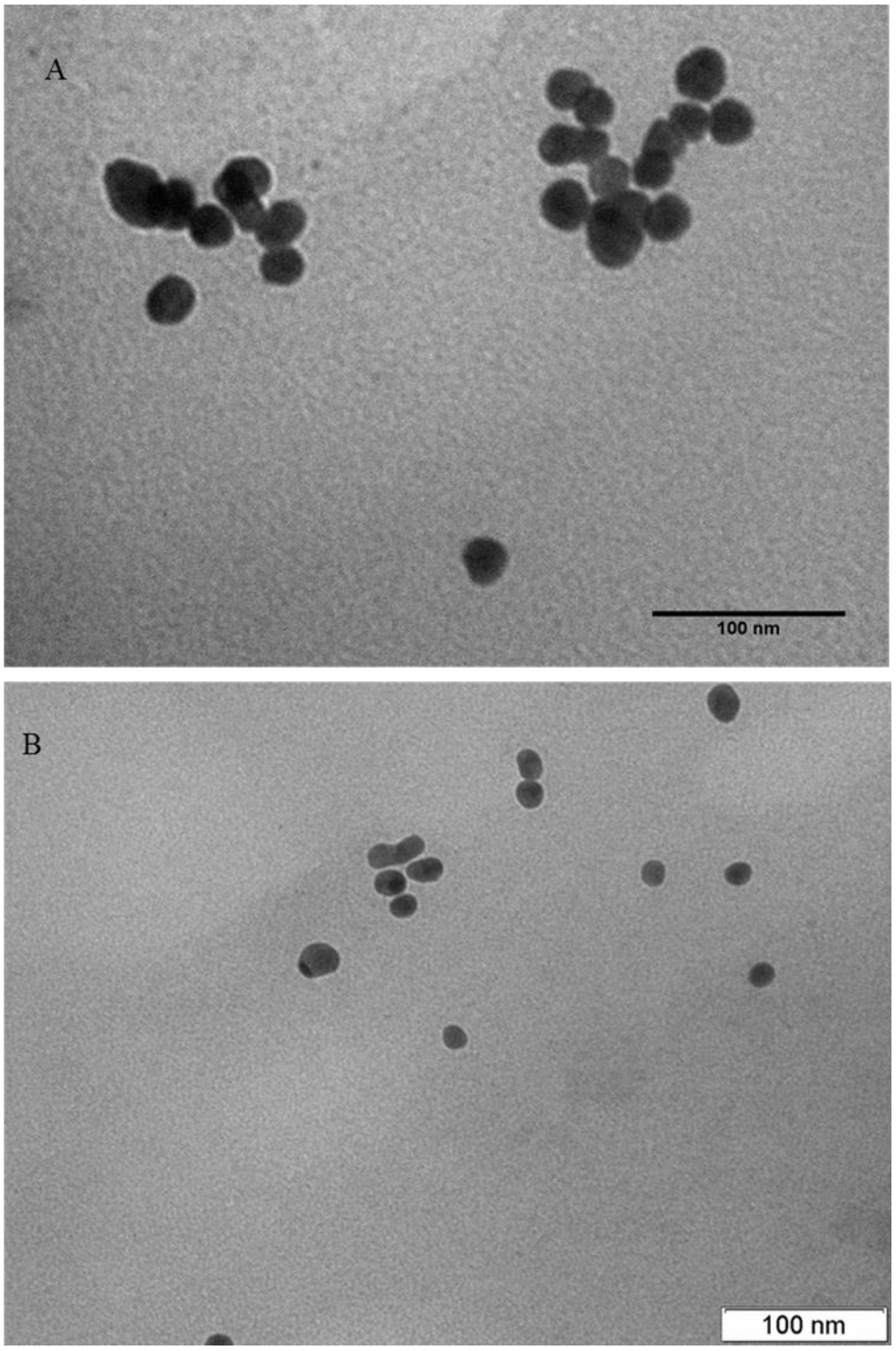

Figure 3.2: Shape and size determination.
TEM images of the citrate AuNPs (A) Particles from a 68 mM citrate reduction (B) Particles from a 136 mM citrate reduction reaction.

The nanoparticle morphology was consistently spherical and exhibited a narrow size distributions (Appendix A1) with some particles as small as 8 nm and as large 20 nm for the 136 mM citrate reduction reaction. However, the particles from the 68 mM citrate reduction were slightly larger, with some as large as 30 nm. This consistency in size and shape was as required for biological application. This was achieved by the use of appropriate levels of the starting material.

The particles were also resolved by HRTEM. HRTEM is used as a confirmatory measure of the crystalline nature of the particles. The images showed distinctly defined lattice fringes (Figure 3.3). The lattice fringes for the various particles were also observed to have different patterns (Figure 3.3). At higher resolution, the presence of a layer around the particles was also evidently visible. This suggests the presence of a layer of citrate on the nanoparticle surface.

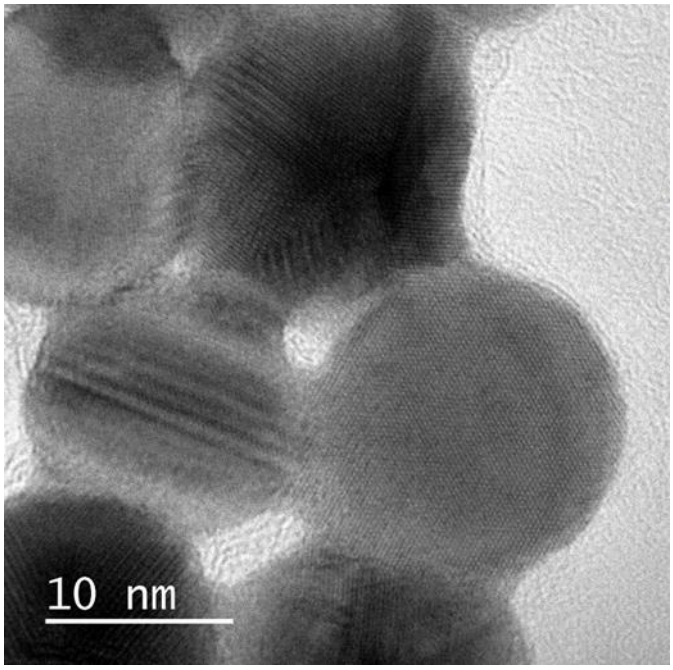

Figure 3.3 HRTEM analysis of citrate capped AuNPs.
HRTEM images of AuNPs. The presence of visibly defined lattice fringes confirmed the crystal morphology of the nanoparticles produced.

3.2 Transmission electron microscopy of bacterial-nanoparticle interactions

E. coli strain BB1553 (MC4100 Δ*dnaK*52*::Cm*^{R} *sidB1)* cells are mutants lacking the *dnaK* gene (Paek and Walker 1987) and, therefore, have a compromised protein folding function. The DnaK protein is essential for cell survival under normal and stressful conditions. The interaction of these cells with citrate coated gold nanoparticles was of interest in light of the DnaK function. This study sought to image the assimilation of AuNPs by *E. coli* Δ*dnaK*52 cells, possible cytotoxicity and structural changes on *E. coli* Δ*dnaK*52 cells caused by citrate AuNPs.

Figures 3.4 and 3.5 show thin sections of *E. coli* Δ*dnaK*52 (*E. coli* DnaK^{-}) and *E. coli* Δ*dnaK*52 that were transformed to express DnaK exogenously (*E. coli* DnaK^{+}) grown in 2YT broth in the presence of citrate AuNPs. Most of the cells viewed were normal in size and had intact cell walls in both *E. coli* DnaK^{+} and *E. coli* DnaK^{-} cells (Figure 3.4A) in comparison to untreated *E. coli* control (Appendix A2). Some cells also appeared elongated with invaginations in the control and the nanoparticle treated cells. Paek and Walker (ibid) reported that *E. coli* Δ*dnaK*52 cells form long filaments in liquid broth due to the lack of DnaK. As reflected by the TEM images, *E. coli* Δ*dnaK*52 was able to internalize citrate AuNPs (Figure 3.4A-D). In all cases AuNPs are seen as black spots within the cell cytosol as indicated by the arrows. Some nanoparticles existed as single species (Figure 3.4A-D), although others were seen to associate as agglomerates or aggregates (Figure 3.4B & D). Single and aggregated AuNPs were also observed outside cells (Appendix A2). Citrate AuNPs were seen to interact with cytoplasmic material (Figure 3.4 B-D) in a manner that might have caused the pulling off of the cytoplasm from the bacterial membrane (Figures 3.4B and 3.4D). The reactions of these AuNPs with the various components could modify the function/activity of the citrate AuNPs within the bacterial cells. These undesirable effects might have resulted in the death of some few cells observed especially in the case of *E. coli* DnaK^{-} cells.

Overall, most of the *E. coli* Δ*dnaK*52 cells tolerated the presence of citrate AuNPs as evidenced by the sustained integrity of their cell structures. Noticeably, citrate AuNPs did not appear to have an effect on the membrane of the *E. coli* cells. Several reports have reiterated on the non-toxic nature to cells of gold nanoparticles of different sizes and capping agents. Anionic gold nanoparticles are reportedly non-toxic unlike cationic particles which interact with charged membrane components thereby disturbing the membrane (Goodman *et al.*, 2004).

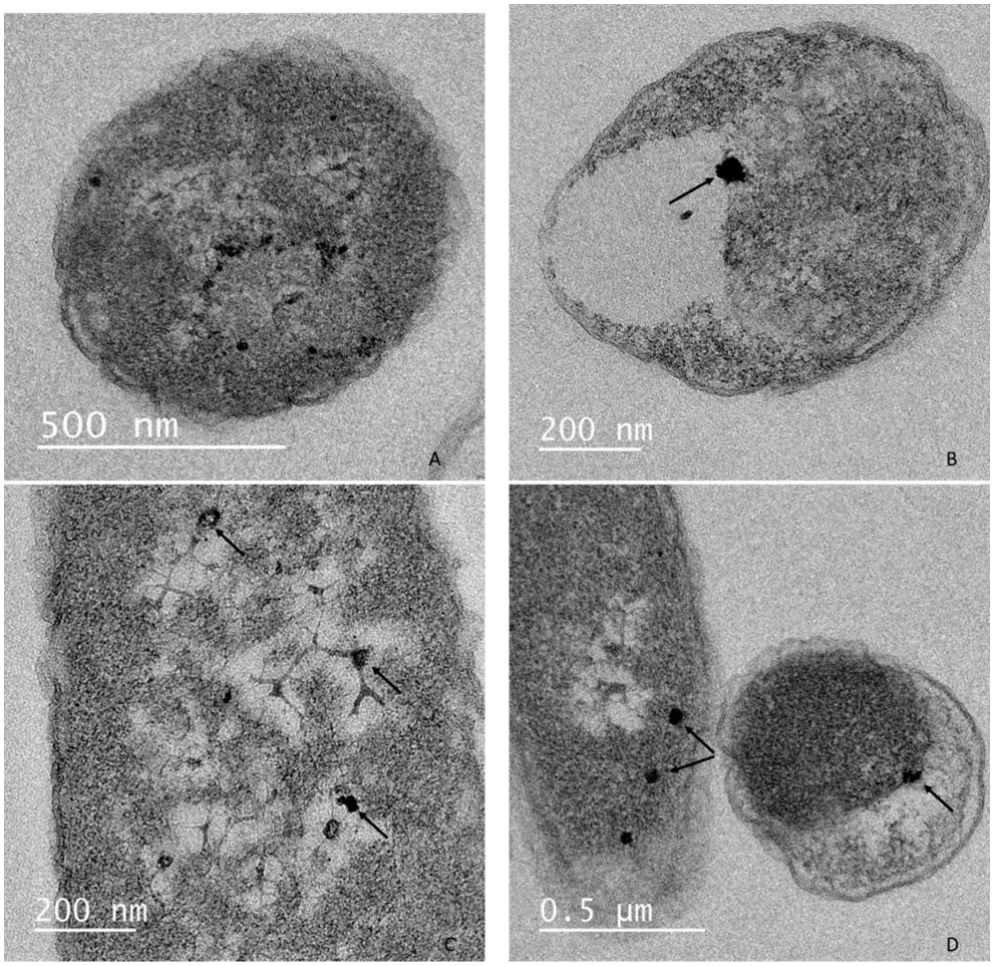

Figure 3.4: TEM images showing *E. coli* Δ*dnaK*52 cells (DnaK$^-$) exposed to citrate-AuNPs. (A) A cell with AuNPs in the cytoplasm, (B) Aggregated AuNPs inside the cell. Cell integrity is compromised, (C) AuNPs inside cell roping up with cytoplasmic material, (D) Cells with aggregated and agglomerated AuNPs showing the plasma membrane that was pulled off the cell wall.

Interestingly, the *E. coli* DnaK^{+} cells exhibited more tolerance to the nanoparticle presence (Figure 3.5). Most of the cells observed still remained intact even in cases were the cytoplasm seemed compromised. The number of dead cells remained minimal in comparison to those observed in the *E. coli* DnaK^{-} cells. This confirms that the DnaK protein played its protective role. Although the AuNPs were reacting or roping up with cytoplasmic material, in certain portions of the cells were the nanoparticles were distributed, patches were observed as indicated by the arrows (Figure 3.5 A-B). The presence of the nanoparticles seemed to be contained by some material that appeared to form a distinct wall in areas in proximity with the NPs within the cell (Figure 3.5). The pulling off of the cytoplasm due to NPs toxicity was evident in *E. coli* DnaK^{-} cells (Figure 3.4 B&D), as opposed to cells expressing DnaK. Thus it is possible that DnaK may have formed part of the 'wall' that cordoned the NPs, preventing them from damaging the cells.

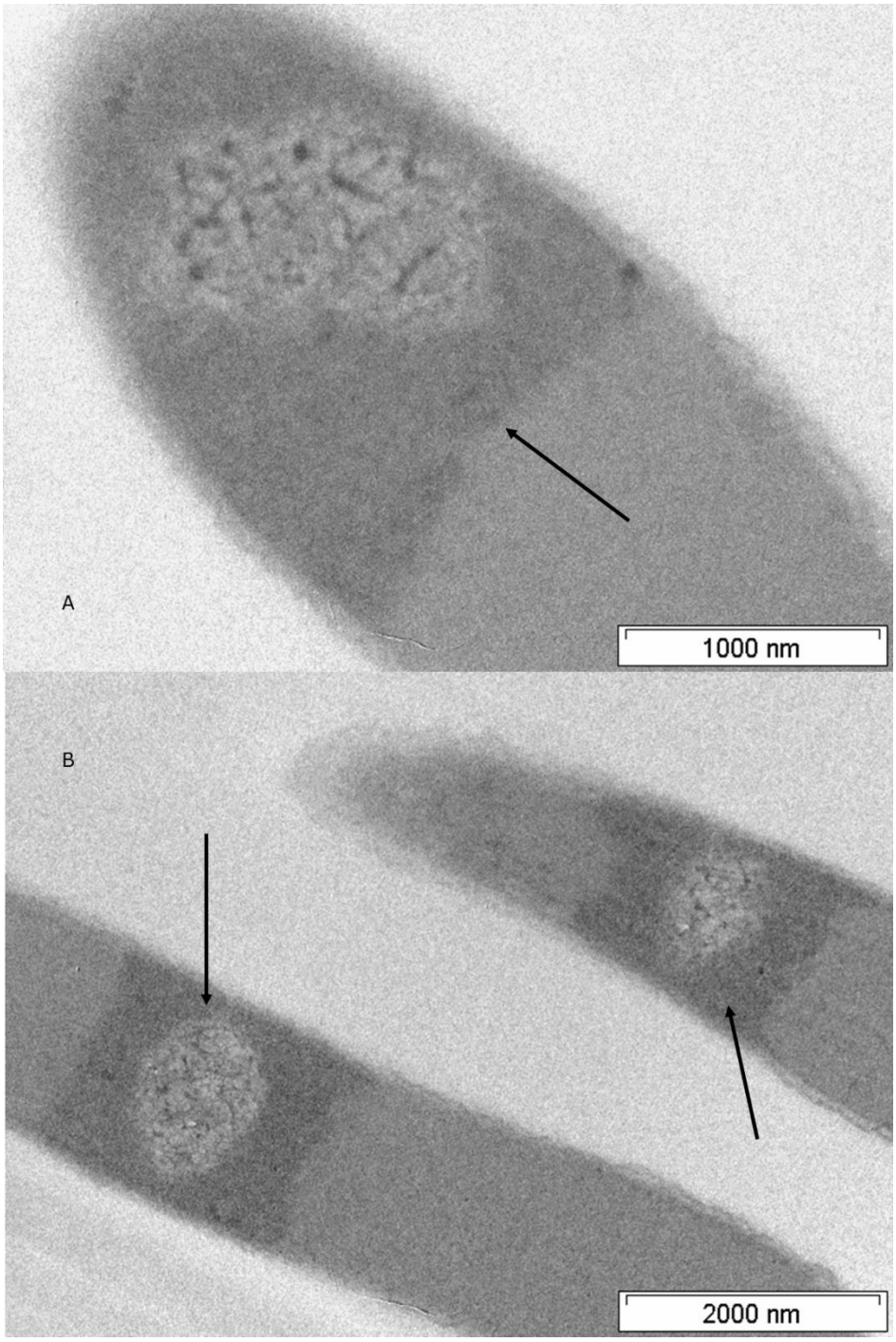

Figure 3.5: TEM images showing *E. coli* Δ*dnaK*52 cells expressing DnaK heterogeneously (DnaK$^+$) exposed to citrate-AuNPs.
(A and B) show how the interaction of AuNPs with cytoplasmic material is contained in DnaK plus cells.

3.3 Effect of citrate gold nanoparticles on bacterial growth

In order to follow up the TEM imaging of *E. coli* Δ*dnaK*52 interactions with citrate AuNPs, it was also of interest to ascertain whether the nanoparticles had any inhibitory effect on *E. coli* Δ*dnaK*52 bacterial growth as different classes of bacteria are said to exhibit different susceptibilities to nanoparticles (Fu *et al*., 2005). The growth of these cells in an environment with nanoparticles was unpredictable given their deficiency of a major house-keeping protein, DnaK.

E. coli Δ*dnaK*52 cells suspended in 2YT were exposed to 25, 50, 75 and 100 µg/mL AuNPs and grown at 30 °C and 40 °C with shaking at 150rpm. Untreated *E. coli* Δ*dnaK*52 cells were used as negative control. At hourly intervals OD_{600} values were monitored from each flask and plotted against time (Figure 3.6). The comparative study on growth of *E. coli* Δ*dnaK*52 under the influence of citrate AuNPs at normal (30 °C) and non-permissive (40 °C) temperatures revealed the effect of the nanoparticles on bacterial growth. The presence of citrate AuNPs reduced bacterial growth insignificantly at 30 °C (Figure 3.4A) and to some notable extent at 40 °C (Figure 3.4B). Under normal growth (30 °C) the *E. coli* curve followed the normal growth trend. With the nanoparticles no particular trend was noticed (Figure 3.4A). Although there is slight reduction of growth at 30 °C in the presence of nanoparticles, there is however no dose dependency in this regard. The curves 25, 50, 75 and 100 µg/mL seemed to follow the *E. coli* growth trend, but only reached OD_{600} 3.4, 3.34, 3.34 and 3.16 at the 5^{th} hour respectively, which was slightly lower compared to OD_{600} 3.5 for *E. coli* at the same hour (Figure 3.4A). This would imply that citrate AuNPs have no net negative effect on the growth of *E. coli.* However, at non-permissive temperature the reduction in growth in the presence of nanoparticles was noticeable (Figure 3.4B). The *E. coli* sample reached OD_{600} 3.41 at the 5^{th} hour which was comparably higher than 2.96, 2.84, 3.06 and 2.79 for the samples treated with 25, 50, 75 and 100 µg/mL respectively (Figure 3.4B). Citrate

AuNPs tend to aggregate in culture media (Figure 3.2 Appendix A2). Particles in aggregates interact less with bacterial cells hence the minimal cytotoxic effects. Generally *E. coli* Δ*dnaK*52 cells seemed to tolerate the presence of up to 100 µg/mL of citrate AuNPs in culture media and this was also supported by data from microscopic studies.

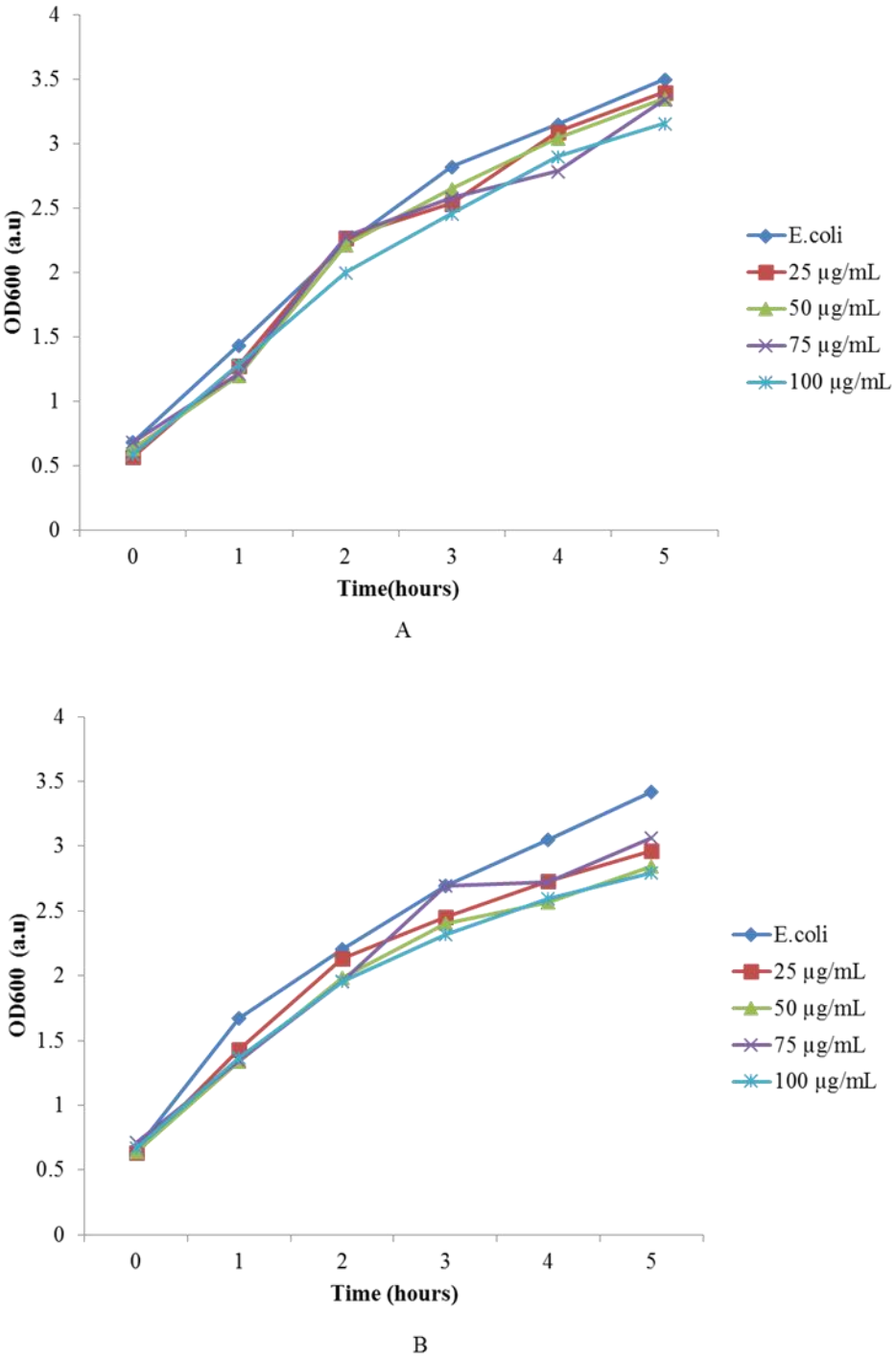

Figure 3.6: The growth curves of *E. coli* under AuNPs influence.
(A) Growth curves at 30 °C and (B) Growth curves at 40 °C. Cells from an overnight culture were grown to OD_{600} 0.6. Cells were exposed to citrate capped AuNPs of concentration 25, 50, 75 and 100 µg/mL. *E. coli* was set as a negative control without nanoparticles. These were incubated with shaking at 150rpm. OD values were noted hourly and plotted.

3.4 Assessment of the capability of gold nanoparticles to suppress protein aggregation in *E. coli*

Mogk *et al* (1999) showed that *E. coli* DnaK mutant cells are prone to heat shock treatment caused by protein aggregation. Such strains are, therefore, temperature sensitive in the absence of DnaK. In their work Shonhai *et al* (2005) were able to demonstrate suppression of thermosensitivity in a DnaK mutant *E. coli* strain *dnaK756* using by heterologous expression of PfHsp70 and its variant, KPf (made up of the ATPase domain of *E. coli* DnaK coupled to the SBD of PfHsp70). The recent revelation of some nanoparticles with chaperone-like properties (De and Rotello, 2008, Luthuli *et al*., 2013) was of interest in light of their protective roles in suppressing protein aggregation. This study sought to introduce citrate AuNPs that were capable of suppressing MDH aggregation *in vitro* (Figures 3.8 and 3.9) into DnaK mutant *E. coli* Δ*dnaK*52 cells and monitor the global protein solubility profiles.

E. coli $DnaK^+$ and *E. coli* $DnaK^-$ cells were exposed to citrate AuNPs in the range '25-75 µg/mL' and incubated at 30 °C and 40 °C in a shaker incubator at 150 rpm for 24 hours. Untreated *E. coli* cells were included as control. Cells were pelleted, lysed and separated into soluble fractions and insoluble fractions by centrifugation at 5000 rpm for 20 min at 4 °C. The samples were analyzed by SDS PAGE.

Figure 3.7 shows the results for the solubility of *E. coli* $DnaK^+$ and *E. coli* $DnaK^-$ proteins in the presence of citrate AuNPs. At 30 °C, in *E. coli* $DnaK^+$ cells, proteins of different sizes were observed in the soluble (S) fraction in the negative control (0 µg/mL) (Figure 3.7 A). The protein at position 70 kDa (marked as DnaK) was expressed in large amounts. This was confirmed by western blotting (Appendix B4). The insoluble (P) fraction also exhibited various bands of

differently sized proteins in the negative control. The amount of DnaK in the insoluble fraction seemed equal to that in the soluble fraction. This showed that DnaK exists as both soluble and insoluble forms. In lanes '25-75 µg/mL', the cells were treated with the varying AuNPs concentrations. The protein profiles were compared to the negative control. It was observed that the proteins profiles were identical to the negative control for both soluble and insoluble fractions across '25-75 µg/mL'. Any noticeable differences in the intensity of some bands was attributed to variable loading effects. On the other hand, Figure 3.7 B shows the protein profiles for *E. coli* DnaK$^-$ cells at 30 °C. Various protein bands were observed in the insoluble fraction in the negative control, with some showing a huge intensity. Several bands were also observed in the soluble fraction of the negative control, but these were fewer and showed less intensity in comparison to the insoluble fraction. One of the bands at position 60 kDa in the soluble fraction was observed to be more intense. In the lanes '25-75 µg/mL' the *E. coli* DnaK$^-$ cells were treated with AuNPs. The protein profiles were observed to be similar to the negative control in both the soluble and insoluble fractions across the nanoparticle concentrations. The intense band at position 60 kDa was also observed in the soluble fraction of the *E. coli* lysate that was harvested from cells that were exposed to '25-75 µg/mL' of nanoparticles. This protein was suspected to be GroEL and was confirmed by Western blotting (Appendix B4). GroEL is an *E. coli* heat shock protein that is essential at all temperatures (Vorderwülbecke *et al.*, 2004). A fraction of the *E. coli* DnaK$^+$ and *E. coli* DnaK$^-$ cells were exposed to the nanoparticles and heat stress at 40 °C. Figure 3.7 (C and D) shows the protein profiles of *E. coli* DnaK$^+$ cells and *E. coli* DnaK$^-$ cells grown at 40 °C in the presence of citrate AuNPs. For *E. coli* DnaK$^+$ cells, in the soluble and insoluble fraction, various bands of proteins were observed in the negative control (0 µg/mL) (Figure 3.7 C). The DnaK protein largely occurred in the soluble fraction in cells that were exposed to heat shock at 40 °C. Cells that were

treated with NPs at concentration '25-75 µg/mL' exhibited protein profiles that bore similarity to the negative control for both soluble and insoluble fractions. This would suggest that the solubility of proteins harvested from *E. coli* $DnaK^+$ was not affected by the citrate AuNPs or possibly DnaK may have acted to suppress protein aggregation.

The protein profiles for the *E. coli* $DnaK^-$ cells at 40 °C are shown in Figure 3.7 D. Several protein bands were observed in the insoluble and soluble fractions in the untreated control (0 µg/mL). Of interest were the huge bands observed, approximately around the 30 kDa and 90 kDa positions (circled in Figure 3.7D), in the soluble fraction at 0 µg/mL AuNPs. These bands were also observed at 30 °C, although there was an up regulation of the proteins at 40 °C. Across the AuNPs concentrations '25-75 µg/mL', SDS-PAGE analysis revealed almost similar protein profiles in comparison to the control with respect to both soluble and insoluble fractions. However, the other two bands (circled) that were observed to be intense in the untreated control (0 µg/mL), appeared less intense across lanes '25-75 µg/mL' in the soluble fractions (Figure 3.7 D). This suggests a shift in the solubility of these two proteins. The presence of citrate AuNPs may have caused the shift of these proteins to the insoluble fractions. On the other hand, based on the sizes of the two protein bands, this may imply that citrate AuNPs interact with either small or large proteins in *E. coli.*

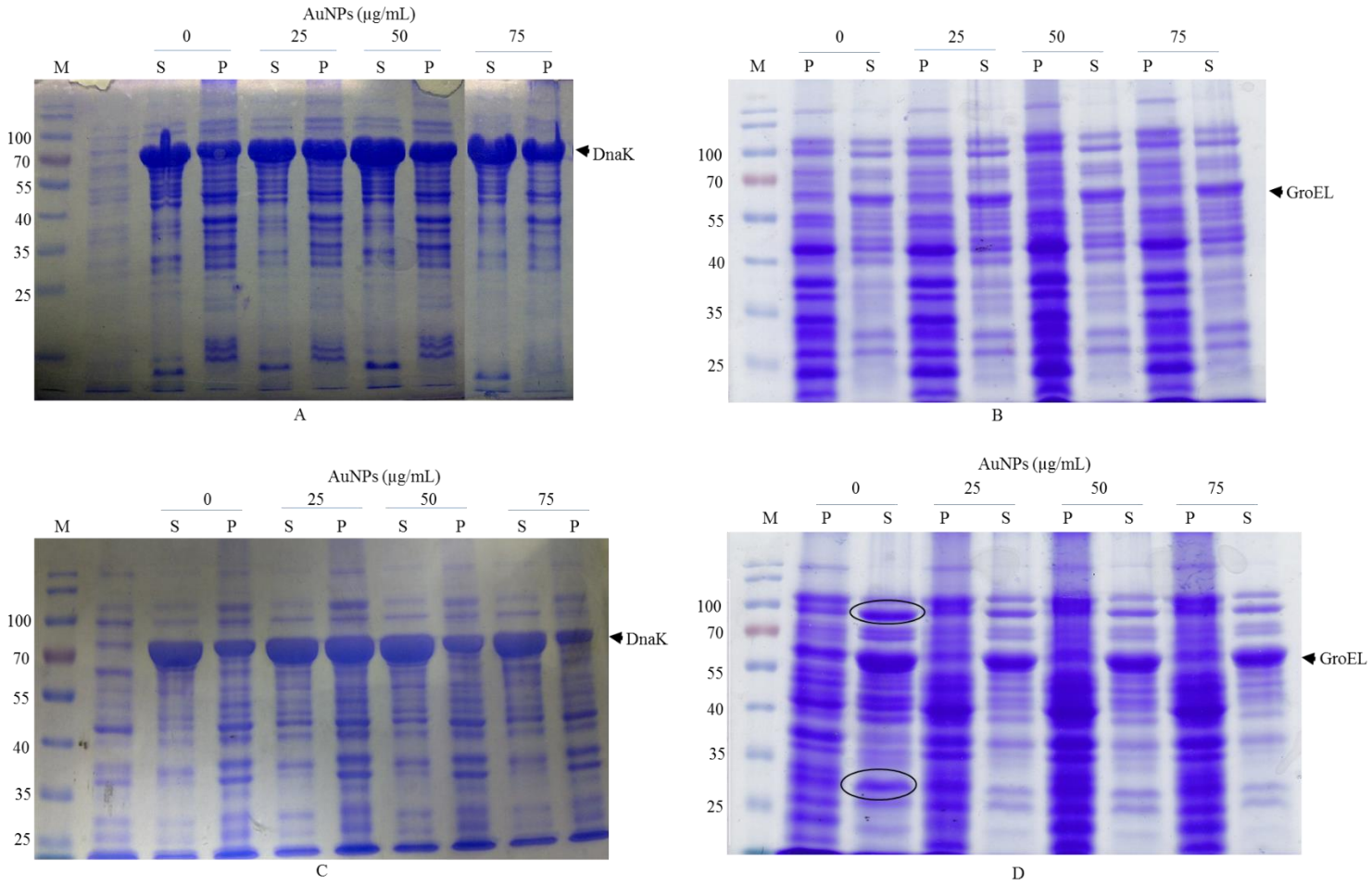

Figure 3.7: Comparison of the protein profiles in *E. coli* Δ*dnaK*52 cells and *E. coli* Δ*dnaK*52 expressing DnaK.
Cells were exposed to 25, 50 and 75 µg/mL citrate AuNPs and incubated overnight at 30 °C and 40 °C. Untreated *E. coli* was used as the negative control. Cells were lysed and pellet and supernatant were separated by centrifugation. Soluble (S) and insoluble (P) fractions were analysed by SDS PAGE. (A) Protein profile for $DnaK^+$ cells at 30 °C. (B) Protein profiles for $DnaK^-$ cells at 30 °C. (C) Protein profiles for $DnaK^+$ cells at 40 °C. (D) Protein profiles for $DnaK^-$ cells at 40 °C.

3.5.1 Citrate gold nanoparticles suppress MDH aggregation and complement the function of PfHsp70 *in vitro*

In this study we investigated the ability of citrate AuNPs to suppress heat induced aggregation of MDH as well as their effect on the activity of PfHsp70, a well-known DnaK homologue (Shonhai *et al*., 2005; 2008).

MDH in the presence of AuNPs and in the additional presence of PfHsp70 was heated to 48 °C and aggregation was measured as an increase in turbidity (Figure 3.8). Untreated MDH aggregated as indicated by a high absorbance value (bar MDH alone, Figure 3.8). MDH is an aggregation prone protein (Shonhai *et al*., 2008) upon exposure to heat stress as indicated by the increase in turbidity over time. In the presence of PfHsp70, MDH aggregation is prevented (bar MDH + PfHsp70, Figure 3.8). In the presence of lower concentrations of AuNPs (2.5-25 µg/mL) MDH aggregation was also prevented in a concentration dependent manner, as shown by low turbidity values (Figure 3.8 A). The low turbidity values as compared to that of untreated MDH confirmed the chaperone-like function of these nanoparticles. However, as concentration increased (50-100 µg/mL), the ability to suppress aggregation by the AuNPs is lost (Figure 3.8 A). This would suggest that at lower concentrations the particles were effective in suppressing MDH aggregation, while this function decreased at higher NP concentration. In the presence of PfHsp70, MDH aggregation was further suppressed by the NPs in a concentration dependent manner. This is evident when compared to the untreated MDH control (Figure 3.8 B); as well as compared to the reaction for MDH exposed to the AuNPs (Figure 3.8A). Lower turbidity values were observed in the additional presence of the PfHsp70 protein in comparison to the PfHsp70 positive control. It is possible that the NPs are cooperating with PfHsp70 in suppressing MDH aggregation.

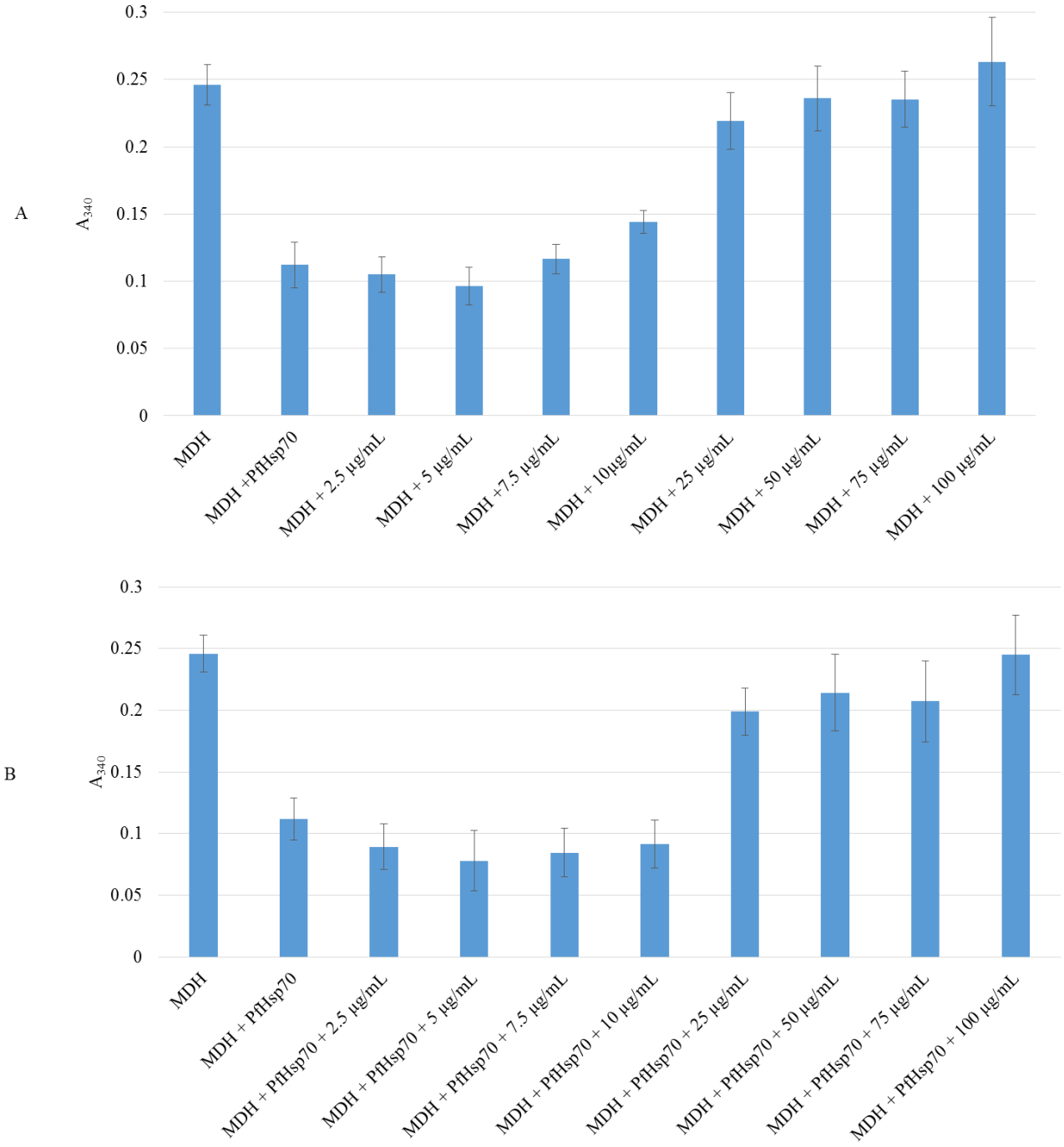

Figure 3.8: **Suppression of MDH aggregation under heat stress**.
MDH alone (negative control). (A) MDH was also treated with AuNPs of concentrations 2.5-100 µg/mL. (B) PfHsp70 was also added to some of the MDH nanoparticle treatments and heated to 48 °C. Absorbance values were measured in triplicate in a 96-well micro titre plate. Data are presented as mean and standard deviation.

3.5.2 Citrate gold nanoparticles maintained MDH in soluble form

Proteins attach or adsorb onto nanoparticle surfaces, altering structure and potential activity of either the nanoparticle or the attached protein molecule (Klein, 2007). This can give rise to either beneficial effects or unpredictable and potentially undesirable effects (Gagner *et al*., 2012). In their study, Luthuli *et al* (2013) showed a potentially beneficial aspect of this adsorption when they showed that cysteine AuNPs maintain MDH is soluble form. This study also sought to investigate the solubility status of MDH in the presence of citrate-AuNPs and in the additional presence of PfHsp70. MDH was mixed with varying concentration of citrate AuNPs and PfHsp70 was also added to some of the MDH-nanoparticle treatments. The solubility of MDH (Figure 3.9) was determined by SDS PAGE analysis.

Figure 3.9 shows the resulted obtained when MDH was incubated at 37 ℃ for 20 mins in the presence PfHsp70, AuNPs and both AuNPs and PfHsp70. Most of the untreated MDH exposed to thermal stress appeared in the insoluble fraction (lane P1, Figure 3.9) and only a negligible amount appeared in the soluble fraction (lane S1, Figure 3.9). As expected, the presence of PfHsp70 promoted the overall occurrence of MDH into the soluble form (lane S2, Figure 3.9; Shonhai *et al*., 2008). However, a lesser amount of MDH appeared insoluble (lane P2, Figure 3.9) even in the presence of PfHsp70. In the presence of citrate AuNPs (lane S3, Figure 3.9) MDH remained in the soluble phase with a smaller proportion of MDH also remaining as insoluble. In comparison to the PfHsp70 control, AuNPs were able to maintain MDH in soluble form. This, however, was in a concentration dependent manner (Appendix A3), with the higher concentrations '25-100µg/mL' being less effective. This could be at higher concentrations the particles aggregated amongst themselves resulting in them presenting surfaces that may have promoted protein aggregation. On the other hand, in the presence of the nanoparticles, PfHsp70 appeared to exhibit improved

function (lane S4, Figure 3). Based on observations, the AuNPs did not interfere with PfHsp70 function and instead they seemed to complement its activity.

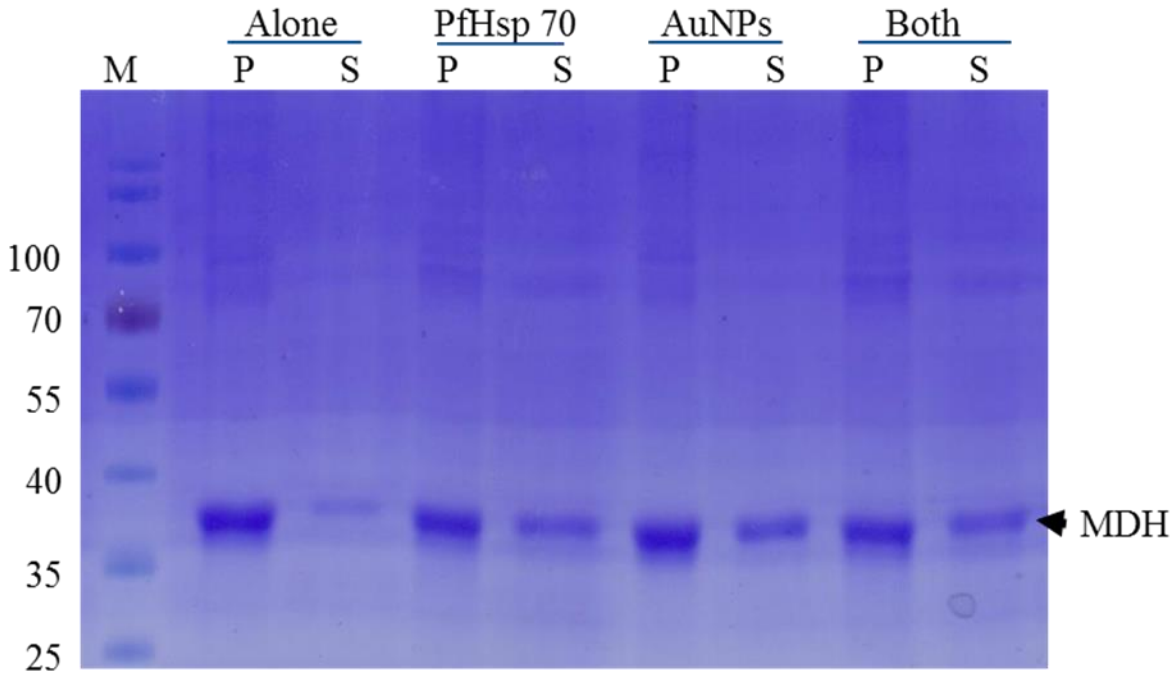

Figure 3.9: Citrate AuNPs maintained MDH in soluble form.
1µM MDH was incubated in the presence of 1.3 µM PfHsp70, in the presence of 10 µg/mL citrate AuNPs concentrations and in the presence of both 10 µg/mL AuNPs and 1.3µM PfHsp70. MDH alone was used a negative control. These treatments were incubated at 48 °C for 20 min. The soluble fraction (S) was separated from aggregated fraction (P) by centrifugation. Samples were analysed by SDS-PAGE.

3.6.1 Citrate gold nanoparticles damage plasmid DNA

Reactions between nanoparticles and biological entities such as proteins and DNA can result in unpredicted and undesirable effects. Damage to DNA can have major deleterious effects to cells and organisms. This study sought to investigate the effects on citrate AuNPs on plasmid DNA since these particles were targeted for biological application in *E. coli*. The study on pQE60/DnaK

integrity in the presence of nanoparticles revealed the effect of these nanoparticles on DNA structural integrity.

The restriction enzyme *Nco* I was used to confirm the integrity of the purified plasmid. The plasmid is 5566 bp and *Nco* I cuts twice at 114 bp and 1323 bp (Figure 3.10A). Two fragments migrating at 1209 bp and 4357 bp were observed (Figure 3.10B). The intact plasmid DNA was exposed to 25, 50, 75 and 100 µg/mL citrate-AuNPs and incubated for 48 hours. Sampling was done at 24 and 48 hours and these were analysed by agarose gel electrophoresis.

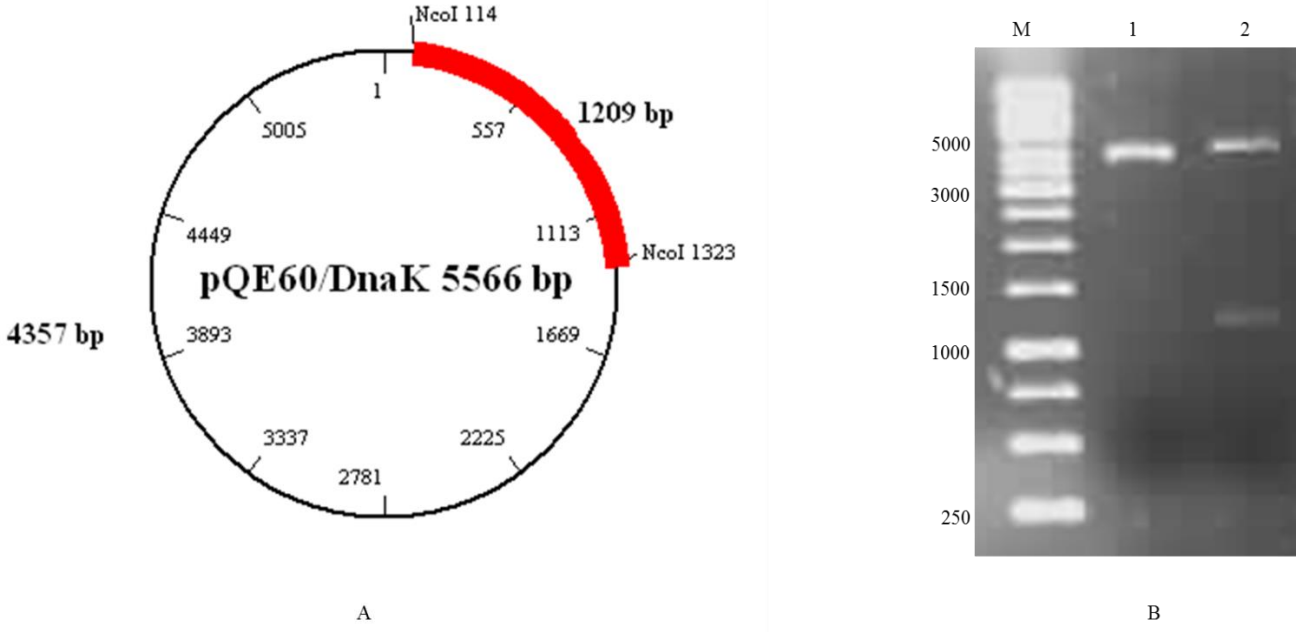

Figure 3.10: Diagnostic restriction of pQE60/DnaK
(A) Restriction map of pQE60/DnaK showing the enzyme *Nco* I used for the restriction digest. (B) Agarose gel electrophoresis of pQE60/DnaK. The loading sequence of the samples was as follows: Lane M: DNA Marker; Lane 1: pQE60/DnaK Uncut: Lane 2: pQE60/DnaK restricted with *Nco* I.

In order to ascertain the effect of citrate AuNPs on DNA structure and stability *in vitro*, plasmid pQE60/DnaK was exposed to 25, 50, 75 and 100 µg/mL. The assay was conducted at 37 °C in a buffer that was at pH 6.6. After 24 and 48 hours, agarose gel analysis was conducted on the DNA samples using a 1.0 % agarose gel and the voltage used was 100 V for 1 hour. Two bands of DNA were observed in the negative control, marked as supercoiled DNA and relaxed DNA, lane N (Figure 3.11). This suggests that the untreated plasmid DNA existed in both supercoiled and relaxed conformations under the prevailing conditions as previously reported (Dunpall *et al.*, 2012). DNA that was treated with titanium dioxide (positive control), Lane P, there were two bands of DNA at similar positions to the bands observed in the negative control. One of the bands marked as supercoiled DNA, indicates the supercoiled covalently closed circular plasmid estimated at just above 5000 bp and the second DNA band, marked as relaxed DNA indicates a larger size of relaxed form of plasmid DNA. For both the negative and positive control, similar results were observed at 24 and 48 hours. This implies that the concentration at which titanium dioxide was used did not cause apparent DNA damage, hence it was an inappropriate positive control.

Figure 3.11, in lanes '25-100 µg/mL', the plasmid DNA was treated with various concentrations of AuNPs. The DNA bands observed in those lanes were compared to the negative control in this experiment. It was observed that across lanes '25-100 µg/mL', there were two bands of DNA present, marked as supercoiled and relaxed DNA (Figure 3.11A). The occurrence of the two bands of DNA in lanes '25-100 µg/mL', in comparison to the negative control, shows that the plasmid DNA had not undergone conformational changes from either the supercoiled or relaxed form. This maintenance of conformation confirmed that citrate AuNPs did not induce any DNA damage to plasmid pQE60/DnaK after 24 hours of exposure (Figure 3.11A).

However, in Figure 3.11 B, lanes '25-100 μg/mL' it was observed that there were now three bands of DNA marked as supercoiled, relaxed and linearized DNA. The existence of the third band across the lanes shows that plasmid DNA had undergone conformational changes from supercoiled or relaxed to a linearized form. This conformational change observed in the lanes '25-100 μg/mL' represents DNA damage. This confirmed that citrate AuNPs induced DNA damage to plasmid pQE60/DnaK after 48 hours of exposure (Figure 3.11B). This implies that plasmid linearization by citrate AuNPs increased with increase in time of exposure. Figure 3.11 B also shows an increase in the intensity of the linearized form of DNA from '25-100 μg/mL'. The intensity of the band indicated the degree/extent of linearization as well showing that damage was concentration dependent.

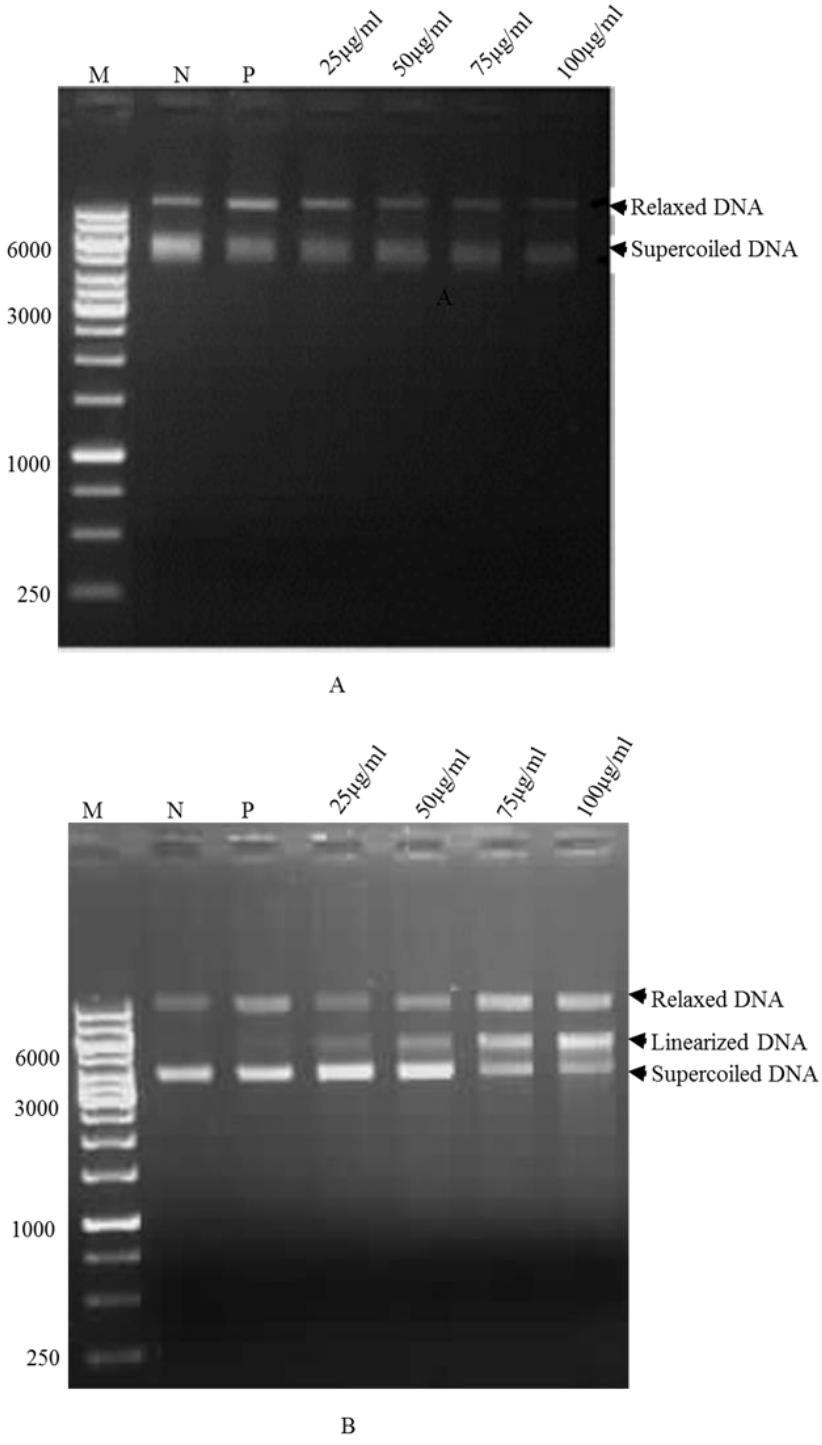

Figure 3.11: The effects of citrate AuNPs on plasmid DNA integrity.
Plasmid pQE60/DnaK was exposed to varying concentration '25-100 µg/mL' of citrate coated AuNPs. The untreated plasmid was used as the negative control and plasmid treated with 1000 µM titanium dioxide as a positive control. The samples were incubated at 37 °C for (A) 24 hours and (B) 48hours. These were analysed by agarose gel electrophoresis.

3.6.2 Transformation of AuNPs-treated DNA into *E. coli* XL1 Blue cells

Plasmid pQE60/DnaK possesses ampicillin resistance and bacteria cells that manage to uptake the plasmid during transformation will ultimately grow on agar supplemented with ampicillin. To confirm DNA damage as a result of the citrate AuNPs, the exposed DNA was transformed into *E. coli* XL1 blue cells and cultured overnight.

The results observed showed the extent to which damage had occurred as this was noted in the number of colony forming units (cfus) in each plate (Figure 3.12). The average number of cfus were numerous in the plates where the cells were transformed with the untreated DNA (negative control) at both 24 and 48 hours (plates A1 and B1, Figure 3.12). This high number of cfus suggests that the transformed DNA was structurally integral. A reduced average number of cfus was noted for the positive control plasmid after transformation from the 24 hour incubations as compared to the negative control (plate A2, Figure 3.12) and yet even lower cfus were noted from the 48 hour DNA transformation (plate B2, Figure 3.12). This suggests DNA damage although this was not visibly evident on the agarose analysis. Transformations with plasmid DNA exposed to 25 – 100 µg/mL for 24 hours generally resulted in numerous cfus showing a similarity to the negative control (plates A1-A6, Figure 3.12). This similarity in the number of cfus to the negative control confirmed the existence of intact plasmid DNA after a 24 hour exposure to citrate AuNPs. However, exposure to 25 µg/mL for 48 hours caused DNA damage as not many cfus were noted as compared to what was observed for the same concentrations at 24 hours as well as the negative control (plate B3, Figure 3.12). The number of cfus were seen to decrease when plasmid DNA from the 50 µg/mL treatment was transformed into *E. coli* (plate B4, Figure 3.12) indicating an increase in the state of damaged DNA. This suggests that there was little DNA to transform cells

and confer ampicillin resistance hence cells died. In this case the number of cfus was taken to represent the extent of damage.

On the other hand, transformations with plasmid DNA exposed to 75 and 100 µg/mL AuNPs for 48 hours resulted in no cfus being noted (plates B5 and B6, Figure 3.12). Plasmid pQE60/DnaK was extensively damaged and failed to transform *E. coli* XL1 Blue cells. *E. coli* XL1 blue cells that were transformed with water (positive control for the transformation) failed to grow on the agar plates. Generally, the failure to transform increased with increase in AuNPs concentration, suggesting that DNA damage by these particles was concentration dependent, agreeing with what was observed in the agarose analysis.

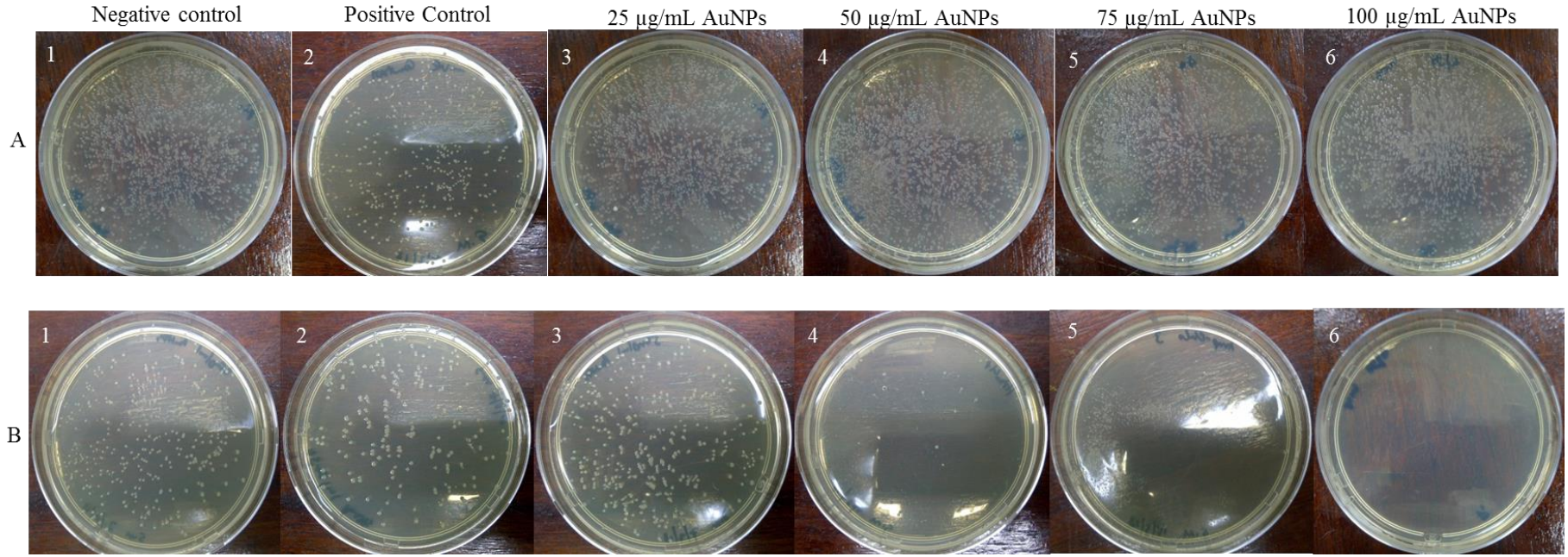

Figure 3.12: Effects of citrate AuNPs on the transformation efficiency of pQE60/DnaK.
E. coli XL1 Blue cells were transformed with plasmid DNA exposed to '25-100 µg/mL' AuNPs for 24 and 48 hours and grown on 2YT agar plates. The plates were imaged and the cfus in each plate were noted. (A) Plates showing cfus of cells transformed with plasmid DNA after 24 hours of exposure. (B) Plates showing cfus of cells transformed with plasmid DNA after 48 hours of exposure.

CHAPTER 4 - Discussion

Synthesis of water soluble citrate AuNPs was achieved using a slightly modified classical citrate method. Sodium citrate tribasic dehydrate was added to reduce the gold as well as cap the resultant nanoparticles since gold has a tendency to form bonds with itself (Sobczak-Kupiec *et al.*, 2011). Sodium citrate was used as it is a common reducing agent (Shipway *et al.*, 2000) although it is known to be a weak reducing agent resulting in large particles (Zhao *et al.*, 2012). Smaller particles can however be obtained through further optimisation of reaction. In this study, the use of an increased concentration of citrate and a low gold salt concentration resulted in the formation of well capped, monodispersed and stable suspensions. High gold salt concentrations have been implicated in causing aggregate formation and leading to turbid solutions. Turbid solutions indicate aggregate formation of different sizes (Tabrizi *et al.*, 2009). The nanosuspensions obtained herein had the characteristic red wine colour.

The red color is due to the surface plasmon resonance (SPR) of the nanoparticles (Ngiem *et al.*, 2010). The nanoparticles showed stability at room temperature over a long time span. The anionic citrate layer on the nanoparticle surface keeps the particles separated minimizing aggregation of the nanoparticles. Citrate also confers a net negative charge on the nanoparticles and is responsible for the AuNPs solubility in water. This would further improve biocompatibility and influences functionality of the AuNPs. In addition, the citrate anions on the AuNPs surface can bond in various ways with different biomolecules under different conditions, hence the use of the AuNPs in various bio-applications.

Characterization of the AuNPs by TEM revealed the monodispersed and spherical nature of the AuNPs. Further analysis by HRTEM showed that the particles were crystalline in nature. The

particles, however, exhibited lattice fringes showing different patterns. These features were of significance especially for further applications in this study.

The citrate AuNPs were then exposed to *E. coli* DnaK^{+} and *E. coli* DnaK^{-} cells. This was to ascertain assimilation and possible effects on growth and physiology. On the other hand, it was also interesting to investigate their effect on the solubility of *E. coli* proteins. *E. coli* is used as a host in heterologous protein production. The yield and solubility of proteins produced in this system is marred by aggregate formations. Introducing AuNPs with chaperone-like properties into *E. coli* could unravel interesting information that can be used in coming up with ways of improving protein solubility in recombinant protein production.

TEM imaging was used to assess the biophysical interactions occurring between *E. coli* DnaK^{+} and *E. coli* DnaK^{-} and the citrate AuNPs. Interactions between bacteria and nanoparticles are said to be governed by the capping agent since the capping agent is responsible for determining surface charge and the chemical properties (Zhou *et al.*, 2012). It has been reported that citrate is a weak capping agent which can easily be replaceable in media solution and hence the nanoparticles tend to aggregate more (Zhou *et al.*, 2012) which limits the nanoparticle bacterial interactions. On the other hand, the tendency to clump together could have resulted from particles reacting with media constituencies on the outside or cellular components on the interior, and these may have replaced the capping agent. This would explain the nanoparticle aggregates observed within and outside the bacterial cells (Section 3, Figure 3.4 B & D) and why some nanoparticles could not enter the bacterial cells. This can further be explained by the fact that the citrate anions gave the AuNPs a net negative charge and bacterial walls also possess a negative charge and hence they tend to repel negatively charged particles. However, McQuillan (2010) reported that electrostatic attraction between anionic nanoparticle surfaces and positively charged regions such as extracellular

domains of integral proteins on *E. coli* could be the primary form of interaction. Hence single and aggregated nanoparticles could have found their way into the cells in this manner without affecting membrane integrity.

On other hand, Kosher (1924) and Skerman (1960) reported that *E. coli* lacks the ability to transfer citrate across its membrane. Therefore, citrate may be excluded as the nanoparticles enter the *E. coli* cytosol (Zhou *et al.*, 2012). Nanoparticles assimilated as uncoated entities are prone to aggregation and unpredictable reactivity, which may explain why the NPs entangled themselves with the cytoplasmic material (Section 3, Figure 3.4 and 3.5). Interestingly, cells expressing heterologous DnaK seemed to have a protective/containment mechanism towards these cytoplasmic reactions with nanoparticles (section 3, Figure 3.5 A-B). In essence this can be attributed to the role of DnaK, a major cellular housekeeper. DnaK is known to prevent and reverse protein misfolding. Thus, the cytoprotective role of DnaK may have reversed the negative effects of the gold NPs on the cells.

Growth studies showed that the various nanoparticle concentrations slightly inhibited bacterial growth at both permissive and non-permissive temperatures. At non-permissive temperatures, thermal stress rather than nanoparticle toxicity could have been responsible for reduced growth rate since the Δ*dnaK52* is known to be thermosensitive (Paek and Walker, 1987). The *E. coli* Δ*dnaK52* strain was reported to grow slowly at 30 °C and to form long filaments at 42 °C (Paek and Walker 1987). Filamentation was reported as possibly accounting, totally or partially for the cell death at 42 °C. Long filaments were also observed during TEM imaging. This could account for the death of some of the cells although the cellular reactions and aggregate formations within the cells could account for the death of other cells. Cui *et al.*, 2012 reported that increased aggregation of nanoparticles within the cell's internal environment increases cytotoxicity.

However, most gold nanoparticles or complexes containing gold have been found to be nontoxic or less toxic to the bacterial system. (Charterjee *et al.*, 2010, Liu *et al.*, 2013). Citrate-AuNPs, at the concentrations used in this study, might therefore, be less cytotoxic and hence inhibit bacterial growth minimally. Similarly Zhou *et al* (2012) using 10 μg/mL as their highest concentration reported that high citrate AuNPs concentrations have a less inhibitory effect on *E. coli* growth. Their argument being citrate AuNPs have a propensity to aggregate and hence particles within aggregates interact less with cells. This would be true for the results obtained in this study as the concentration range used '25-100 μg/mL' was even higher than what Zhou *et al* (ibid) used.

The *E. coli* Δ*dnaK*52 strain is stress sensitive due to the lack of DnaK although plasmids with the dnaK gene can be introduced into it to reverse this. Incubation of the cells at 42 °C is reported to have resulted in aggregation of ~10 % of the soluble proteins in just 60 minutes (Mogk *et al.*, 1999). Introducing chaperone-like citrate-AuNPs into Δ*dnaK52* did not alter the protein profiles of the cells both at normal growth and heat shock conditions in $DnaK^+$ cells (section 3, Figure 3.7A and C). However, any changes in the solubility of the proteins could have been reversed by the DnaK protein as it plays many cellular protective roles. This seemed to agree with what was observed in TEM imaging of $DnaK^+$ cells in the presence of AuNPs. TEM imaging revealed this protective role of DnaK in $DnaK^+$ cells as roping up of citrate AuNPs with cytoplasmic material was contained in the presence of DnaK (section 3, Figure 3.5 A-B). Moreover, the apparent lack of protein aggregation in heat stressed cells that transformed with plasmid DNA expressing DnaK shows that citrate AuNPs do not interfere with the function of DnaK. In addition, this suggests that the NPs do not influence the solubility of DnaK itself.

In DnaK$^-$ cells the protein profiles were not changed due to the nanoparticle presence (secttion3, Figure 3.7 B and D). There was, however, a noticeable increase in synthesis of some proteins at 40 °C, and this was due to the heat shock response. Paek and Walker (1987) reported that the Δ*dnaK52* mutant showed a high basal level of synthesis of heat shock proteins, GroES and GroEL among others after being shifted to 42 °C. GroEL was confirmed as the band at 60 kDa by western blotting. However, this band was not present in *E. coli* DnaK$^+$ cells that were exposed to the NPs as well as heat stress. This may suggest that GroEL may functionally substitute DnaK function under stressful conditions (Vorderwülbecke *et al.*, 2004).

However, neither this noticeable high level synthesis of Hsps nor the presence of chaperone-like AuNPs altered the solubility of most proteins that were expressed by the *E. coli* Δ*dnaK52* DnaK$^-$ cells. Although the nanoparticles showed capability to suppress MDH aggregation *in vitro* (section 3, Figures 3.8 and 3.9) as well as their ability to enter the *E. coli* cytosol, the particles did not influence solubility of *E. coli* proteins. Two protein bands were observed to have shifted from soluble to insoluble in DnaK$^-$ cells in the presence of AuNPs (section3, Figure 3.7 D). This aggregation may be attributed to the nanoparticles and with the DnaK function missing, this aggregation could not be reversed even though the cells expressed another *E. coli* chaperone, GroEL. This could be attributed to non-specific reactions. It is also possible that the nanoparticles may have roped up with proteins by first interacting with other materials such as DNA forming aggregates. Then once such aggregates were formed then they roped up with the rest of the cytoplasmic material. Roping up of cytoplasmic material with the nanoparticles was observed by TEM imaging. Also evident from the TEM images was the existence of the nanoparticles as aggregates. It is possible to assume that nanoparticles in aggregates may or may not actively interact with *E. coli* Δ*dnaK52* proteins and hence impact on protein solubility. Also given the

approximate sizes of the two proteins, 30 kDa and 90 kDa (section 3, Figure 3.7 D), this gives the implication that nanoparticles interact with proteins of any size, large or small given their high protein adsorptive properties. However, this protein-nanoparticle interaction might result in aggregation of the protein as was observed with these two proteins in *E.coli* DnaK^{-} cells at 40 °C.

In their studies Mogk *et al* (1999) reported that only the DnaK protein folding pathway efficiently reversed protein aggregation in heat treated *E. coli* Δ*dnaK52* cells. Furthermore, Bukau and Walker (1990) also reported that the missing function of the DnaK system cannot be replaced *in vivo* by other chaperones. Citrate-AuNPs in the *E. coli* cytosol could have been less effective in reversing protein aggregation and could not match up to the role of DnaK. Also given the overcrowded cellular environment the nanoparticles could have preferentially reacted with other cellular components. This could have inhibited or altered the desired function of the nanoparticles resulting in the roping up of nanoparticles and material as evidenced by TEM imaging. On the other hand, although *E. coli* Δ*dnaK52* cells were suitable for studying protein folding because of the lack of DnaK other functions were speculated to be defective at 30 °C (Bukau and Walker 1989). Hence the results observed might not be a true reflection of what the nanoparticles can do *in vivo* but an influence of the other cellular defects. In this case, the gold nanoparticle function on protein solubility *in vivo* would then be difficult to ascertain as compared to *in vitro*. This might be a good indicator as to the choice of cells used and in this regard further elucidation is needed using *E. coli* cells that only have a defective DnaK function.

MDH was adopted to investigate the capability of citrate-AuNPs in suppressing aggregation *in vitro*. This study also further investigated the effect of the nanoparticles on PfHsp70 suppression of aggregation. MDH is an aggregation prone protein and chaperones are known to suppress its aggregation at 48 °C (Shonhai *et al.*, 2008). In their work Luthuli *et al.*, 2013 showed that cysteine

AuNPs protected MDH from aggregation and De and Rotello (2008) reported that 2-(10-mercaptodecyl)malonic acid coated AuNPs refolded thermally denatured chymotrypsin, lysozyme and papain.

As expected MDH alone aggregated and its aggregation in the presence of PfHsp70 was suppressed (Section 3, Figure 3.8). Upon exposing MDH to heat in the presence of citrate-AuNPs, suppression of aggregation was concentration dependent. Lower order concentrations suppressed aggregation whereas high concentrations were less effective. In lower order concentrations the nanoparticles may have existed as single species or smaller aggregates free to interact with the protein. At much higher order concentrations '25-100 μg/mL', the citrate-AuNPs tend to form large aggregates which contain multiple monodispersed nanoparticles (Zhou *et al.*, 2012). This would present a large surface area which would lead to perturbation of protein structure (Fei and Perret, 2009). The chaperone-like properties of citrate-AuNPs can only be confirmed for lower order concentrations.

Furthermore, it was observed that suppression of MDH aggregation by PfHsp70 in the presence of AuNPs, in comparison to the negative control (MDH alone) or in comparison to the MDH plus nanoparticles, is further reduced in line with what Luthuli *et al* (2013) observed, that cysteine capped AuNPs improved the chaperone function of human heat shock protein 70. Structural similarities between hHsp70 and PfHsp70, irrespective of the different capping agents used and the different nanoparticle concentrations, might have attributed to the similarity in the results of this study and those obtained by Luthuli *et al.* This suggests that citrate AuNPs, at lower concentrations '2.5-10 μg/mL', complement the PfHsp70 function resulting better suppression of aggregation. Alternatively this findings from the current study might be explained in terms of preferential binding. In solution MDH may either prefer binding to the PfHsp70 protein or to the

citrate AuNPs. Be it as it may, the net effect from the data confirms that both PfHsp70 and the NPs promote the stability of MDH (section 3, Figure 3.8).

Insoluble MDH was precipitated when MDH was exposed to 48 °C for 20 minutes (Section 3, Figure 3.9). In the presence of PfHsp70 and the nanoparticles, a fraction of the protein remained soluble supporting data from the turbidity measurements. It is also interesting to note that Luthuli *et al.*, 2013 reported that cysteine AuNPs protected MDH and citrate synthase (CS) from heat induced aggregation, confirming the chaperone-like function. However, in the presence of nanoparticles, it can be argued that some of the protein that sedimented in the pellet fraction may not necessarily have been insoluble. Nanoparticles exhibit high protein adsorptive capacities (Horie *et al.*, 2009) and bind to proteins in different ways via hydrophobic interactions, electrostatic interactions etc. (Patil *et al.*, 2007). In this case binding of citrate-AuNPs to heat stressed MDH prevented aggregation, but it is also a possibility that some of the protein bound to nanoparticles could have pelleted together with the nanoparticles into the insoluble fraction during centrifugation. This sedimentation may have been thus promoted by the extra mass of the nanoparticle added to the protein.

Zaqout *et al* (2012) in their work managed to recover lactate dehydrogenase (LDH) from the TiO_2 nanoparticles to which it had been adsorbed. They then carried out LDH activity assays which showed that the protein was still active despite being initially associating with the NPs and sedimenting as an insoluble fraction. Hence the association of protein to form insoluble aggregates does not necessarily suggest that the protein's structural-functional features are compromised. In the study by Zaqout *et al* (2012), it can be speculated that the conformational changes were reversible and the protein reverted to native conformation on removal of the nanoparticles. However, the current study did not assess the activity of the MDH that was bound to the NPs.

Alternatively, it is also possible conformational changes of adsorbed protein might have seeded further protein aggregation through interactions with proteins in solution (Zhang *et al.*, 2009). In their work, Zhang *et al* (2009) reported that aggregated proteins in solution or aggregates that fall off from the AuNPs surface act as nucleation sites for the formation of more aggregates. This may explain the greater proportion of MDH that precipitated in the insoluble fraction. In the presence of both AuNPs and PfHsp70, also a fraction of MDH remained soluble (Section 3, Figure 3.9). This follows the dynamics of the interactions happening between PfHsp70 – MDH, PfHsp70 – AuNPs, PfHsp70 – AuNPs – MDH and AuNPs – MDH. Once these dynamics are fully understood, nanoparticles can be used in combination with Hsps in improving protein solubility.

In order to address genotoxicity concerns of the citrate-AuNPs, their interaction with DNA was assessed using agarose gel electrophoresis and confirmed by transformation into *E. coli* XL1 blue cells. DNA can assume different confirmations under different conditions and this has an effect on its gel mobility when subjected to agarose gel analysis.

Citrate-AuNPs at the concentrations '25-100 μg/mL' were non-damaging to DNA at 24 hours. Damage was only evident after 48 hours at the same nanoparticle concentrations. The results at 24 and 48 hours revealed that longer exposure time in the presence of citrate-AuNPs causes DNA damage (Section 3, Figure 3.11). Nanoparticles introduced into a system may have longer residence times and only then can their effect be seen. On the other hand, citrate-AuNPs caused DNA damage in a concentration dependent manner across '25-100 μg/mL'. This means as concentration increases, there are more particles in solution to interact with DNA molecules. The apparent DNA damage observed at concentrations '25-100 μg/mL' after 48 hours could have been a result of interaction with the AuNPs or due to formation of reactive oxygen species (ROS), but

direct or indirect interaction of nanoparticles with DNA results in varying biological and biochemical effects, leading to mutations and genomic instability (Li *et al*., 2010).

Bacteria cells transformed with plasmid DNA pQE60/DnaK took up the plasmid and were able to grow on media supplemented with ampicillin, to which the plasmid offers resistance (Section 3, Figure 3.12), hence more transformants were observed. In cases where the plasmid was damaged no resistance was conferred and hence no or less transformants/colony forming units were observed on media plates (Section 3, Figure 3.12). The observed DNA damage due to the citrate-AuNPs presents a possible biosafety concern. It is also a possibility that the nanoparticles might influence transformation of plasmid DNA. Toxicity to *E. coli* competent cells by the nanoparticles may result in no or fewer transformants. Conversely, nanoparticles may bind DNA, transport it across the bacterial membrane and deposit it inside the cell thereby improving transformation efficiency.

CHAPTER 5 – Conclusion

5.1 Conclusion and future work

Overall, this study observed that AuNPs are taken up by *E. coli* cells. The NPs do not appear to be toxic to cells that have an integral protein folding system. However, in the absence of DnaK, the *E. coli* cells fail to contain the nanoparticle presence and exhibit signs of cytotoxicity.

The fact that *E.coli* internalized and tolerated the AuNPs could be a promising aspect in the prospect of using synthetic nanoparticles as molecular chaperones to improve the production of soluble recombinant proteins in *E.coli*. However, further studies need to be done to investigate appropriate growth conditions towards exploring the effects of AuNPs on E. coli protein integrity. Citrate AuNPs seemed to interact with both MDH and PfHsp 70, suppressing aggregation of the former and complementing the activity of the latter. This suggests that gold nanoparticles may complement the role of molecular chaperones in E. coli.

In future, an investigation into the phenomenon behind the way in which *E.coli* $DnaK^+$ contained the effects of AuNPs in the cytoplasm would be important. It will be interesting to unveil the mechanism behind the formation of patches in nanoparticle affected areas. Such a study would divulge important information on the interaction of nanoparticles and the DnaK and how this might impact on protein folding in *E.coli*.

Appendix A - Supplementary data

A1. Size distribution for the citrate AuNPs

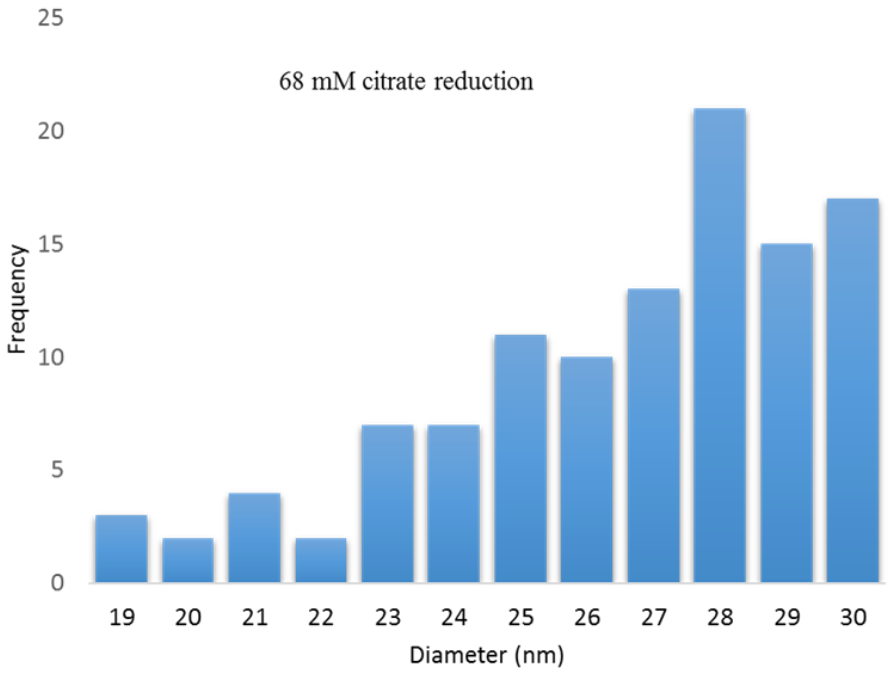

A

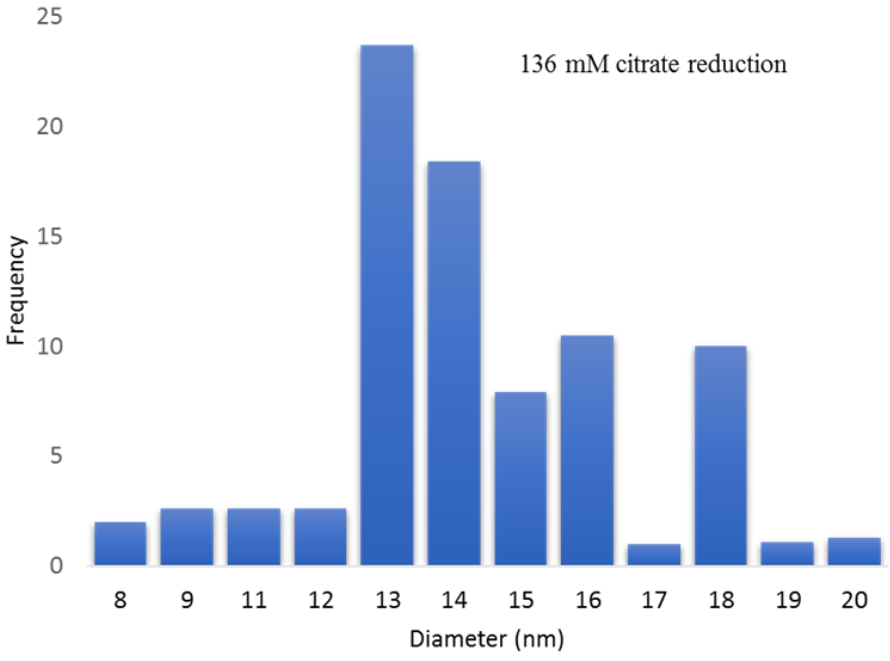

B

A2. TEM of bacterial-nanoparticle interactions

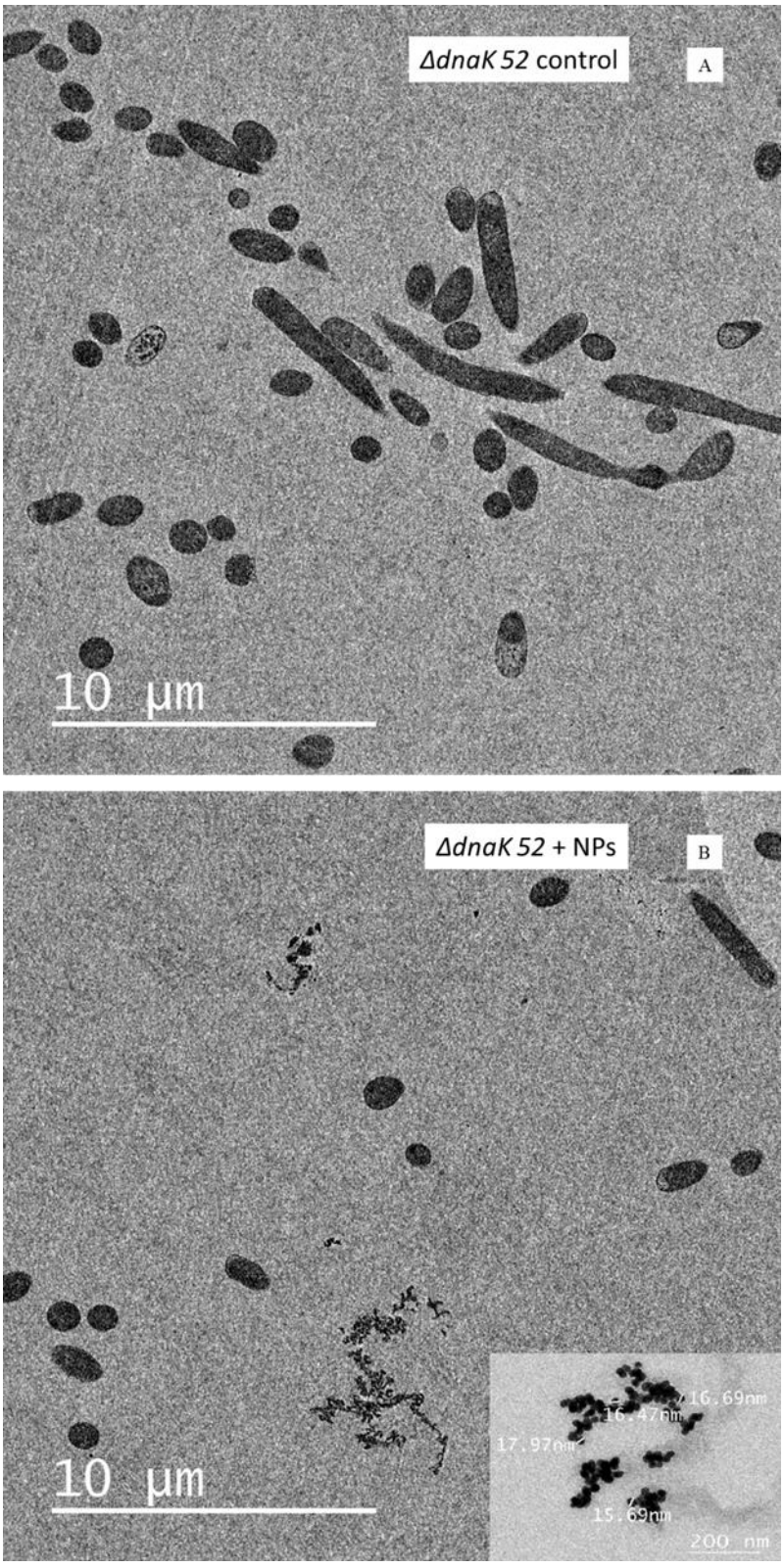

A3. Solubility of MDH in the presence of lower and higher concentrations of citrate-AuNPs

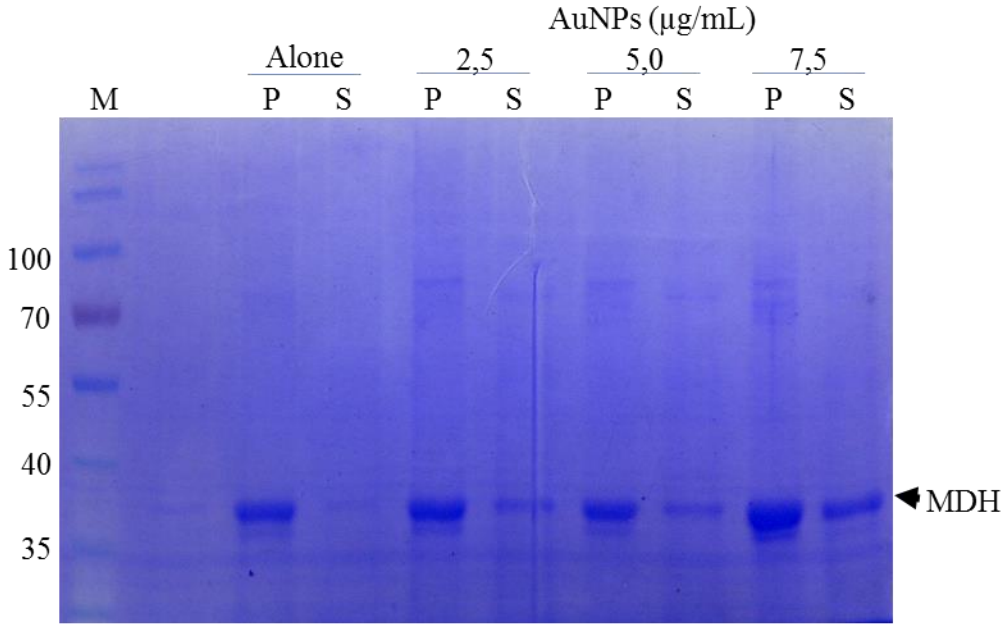

A

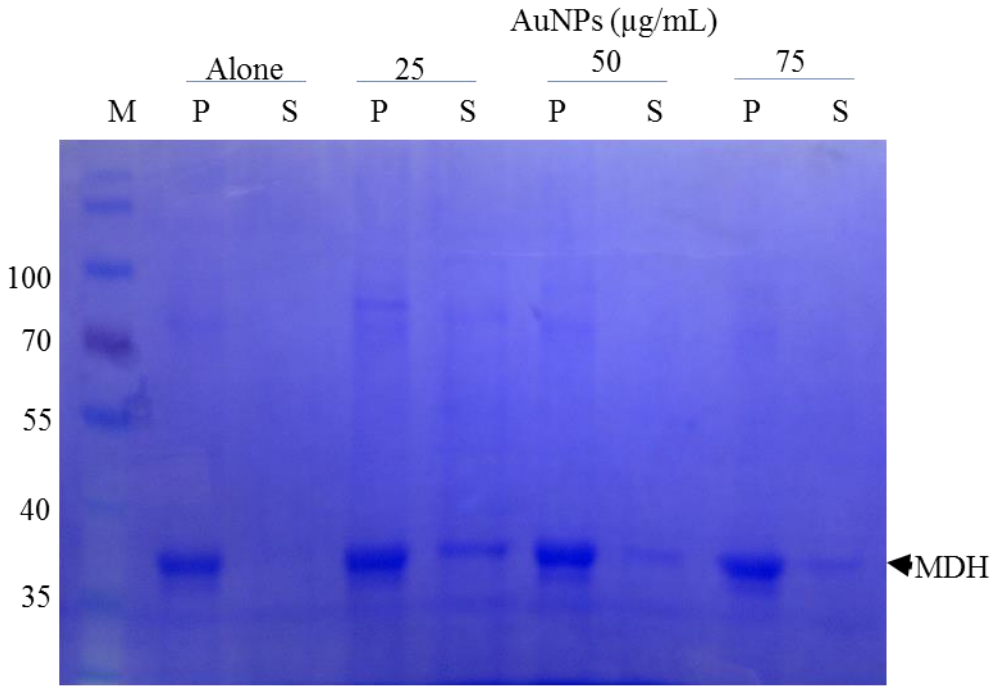

B

Appendix B – General Procedures

B1. Sodium dodecyl polyacrylamide gel electrophoresis (SDS-PAGE)

All electrophoresis was conducted using the Bio-Rad Mini protein 3 electrophoresis system (Biorad, U.S.A). Preparation of the running and stacking buffers was carried out as shown (Appendix B). Gels were allowed to stand for 15 minutes for the polymerisation to complete. They were then transferred into the electrophoresis tank with electrophoresis buffer (25 mM Tris, pH 8.3 250 mM glycine and 0.1 % (w/v) SDS) was added. Protein samples for analysis were mixed with SDS sample buffer (0.25 % Coomasie Brilliant blue (R250); 2 % SDS; 10 % glycerol (v/v); 100 mM tris; 1 % mercaptoethanol) in a ratio of 4 : 1, boiled for approximately 10 minutes and loaded into gel wells. Bio-Rad premixed molecular weight markers were also loaded. The electrophoresis was allowed to run for 90 minutes at 120 volts, unless stated otherwise.

Table B.1 Solutions for making a 5 % stacking gel and a 12 % resolving gel for SDS-PAGE

Reagent (ml)	5 % stacking gel	12 % resolving gel
Distilled water	2.1	3.16
30 % polyacrylamide	0.470	4.16
1.5 M Tris (pH 8.8)	-	2.5
1.0 M Tris (pH 6.8)	0.875	-
10 % SDS	0.035	0.100
10 % Ammonium persulphate	0.0175	0.050
TEMED	0.020	0.020
Total volume	3.5 ml	10 ml

Table B.2 5x SDS running buffer

Reagent (g)	1000 mL
Tris	15.125
Glycine	72
SDS	5

Make up to 1 litre with double distilled water

Table B.3 SDS sample buffer

mL	8.0
Deionised water	3.8
0.5M Tris pH 6.8	1.0
Glycerol	0.8
10% SDS	1.6
2Mercaptoethanol	0.4
1% Bromophenol blue	0.4

B2. Purification of His-Tagged PfHsp70

The following is a summary of the steps used for the purification of PfHsp70

1. An apprpopriate volume of Ni-NTA was added into a tube and centrifuged for 2 minutes at 700 x g.
2. Two resin bed volumes of equilibration buffer were added and mixed until resin was fully suspended.
3. Cenrifugation was done for 2 minutes and supernatant discarded.
4. The sample was prepared by mixing protein extract wiht an equal volume of equilibration buffer. The total volume was twice the volume of the resin.

5. The protien extract was added to the resin and mixed on a shaker for 30 minutes.
6. This was the centrifuged for and some supernatant saved for downstream analysis.
7. The resin was washed with two-resin bed volumes of wash buffer and centrifuged. The was step was repeated and the supernatant saved for analysis.
8. The bound His-tagged protein was eluted using one resin-bed volume elution buffer. Centrifugation was at 700 x g for 2 minutes. The elution step was repeated and in each case the supernatant saved sepaerately.

B3. Western blotting analysis of proteins

On completion of electrophoresis, SDS-PAGE gels were removed from glass plates and the stacking gel cut off. The gel; 3 mm Whatman filter papers, two Scotchbrite fibre pads and nitrocellulose western transfer paper (Hybond-C extra, ECL; Amersham, U.S.A) were immersed in ice cold western transfer buffer (25 mM Tris; 192 mM glycine 159 and 20 % methanol) to equilibrate for about 15 minutes. The gel was then placed on the filter paper on top of the Scotchbrite pad. The nitrocellulose paper was then laid over the gel, followed by the filter paper and the other Scotchbrite pad. All air bubbles were expelled by pressing the sandwich gently upon which the transfer sandwich was placed in the transfer holder in such a way that proteins will migrate towards the nitrocellulose membrane. An ice pack was placed next to the holder to keep the transfer cool. The transfer was run at 100 volts for 1 hour.

B4. Visualisation of Western blots

The production of the His-tagged PfHsp 70 was confirmed using anti-His antibodies (Thermoscientific, U.S.A) and monoclonal antibodies specific for PfHsp 70 respectively. For the confirmation of DnaK and GroEL, anti-DnaK and anti-Hsp60 primary antibodies were used and a

goat anti-rabbit secondary antibody was used. ECL was employed for chemiluminscence-based immunodetection. The membrane was blocked for 1 hour using 5 % non-fat milk in TBS. This was followed by incubation with the primary antibody (dilution ratio 1 µL of antibody to 3000 µL of milk) for overnight. The membrane was washed three times using TBS-Tween (TBS + 0.1 % tween 20) for 15 minutes each wash. The membrane was then incubated with the secondary antibody (dilution ratio 1 µL antibody to 2000 µL of non-fat milk) for 2 hours. The membrane was washed at least 3 times using TBS-Tween. The Western blots were developed onto x-ray film for visualization using the ECL and hydrogen peroxide in a dark room.

B5. Bradford assay

1. Standard solutions of concentrations 5, 10, 15, 20, 25 and 30 µg/mL were made up to 100 mL with PBS.
2. 900 µL of Bradford reagent was added to each sample.
3. The solutions were vortexed and left to stand for 15 min.
4. Absorbance was measured at 595 nm.
5. 100 µL PBS + 900 µL Bradford was used as blank. Readings were recorded in triplicate and mean values were used to plot a curve.

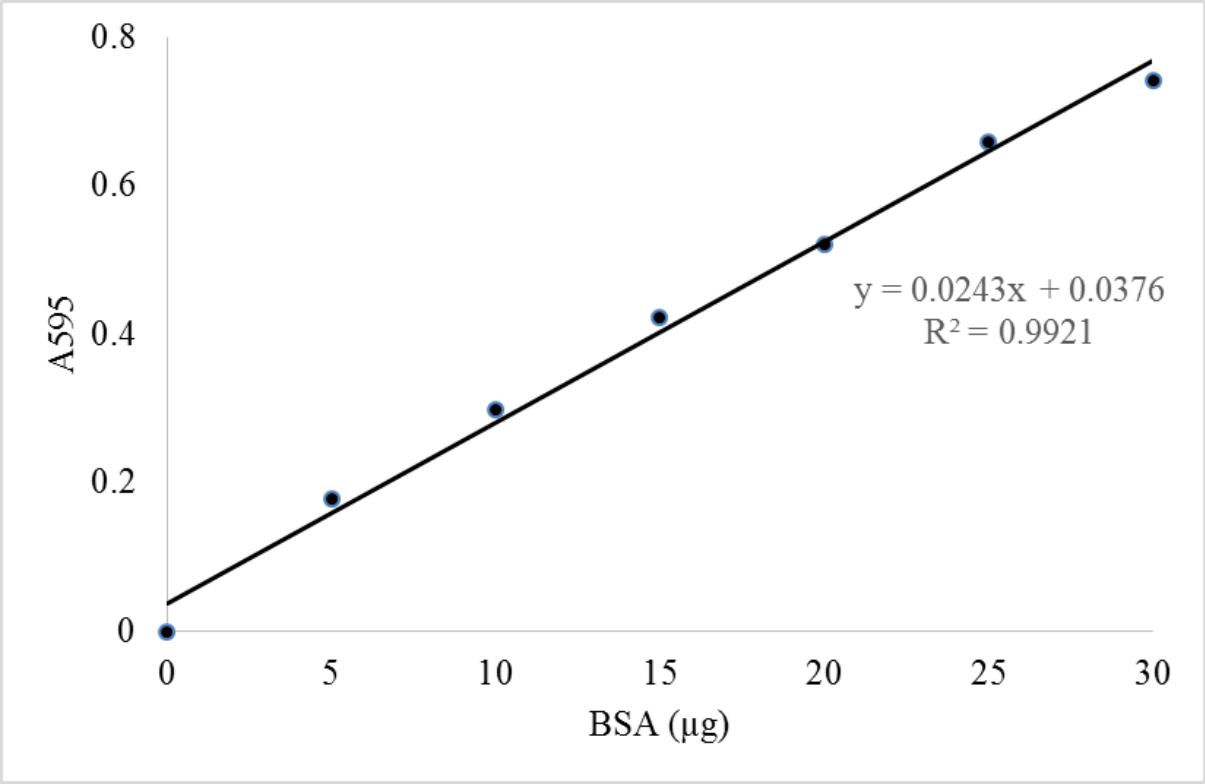

Figure B1. Bradford assay standard curve

Sample preparation.

1. 10 µL of sample was mixed with 90 µL of PBS.
2. 900 µL of Bradford reagent was added.
3. This was vortexed and left for 15 minutes**.**

B6. DNA purification

The pellet was re-suspended in 200 µL of P1 buffer by vortexing. To this 200 µL of P2 buffer was added and the tube was inverted 4–6 times to mix for about 2 minutes. Cell lysis was complete when the solution appeared clear, purple and viscous. 400 µL of P3 buffer was added and mix gently but thoroughly until the sample turned yellow to indicate completion of neutralisation. The sample was centrifuged for 3 minutes. The supernatant was transferred into a Zymo-Spin™ IIN column in a collection tube. Care was taken not to disturb the green pellet to avoid transfer of any

cellular debris into the column. The Zymo-Spin™ IIN/Collection tube assembly was centrifuged for 30 seconds and the flow through discarded from the collection tube. 200 µL of Endo-Wash buffer was added to the column and centrifuged for 15 seconds, followed by addition of 400 µL of Plasmid wash buffer and centrifuging for 30 seconds. The column was then transferred to a clean 1.5 mL microcentrifuge tube. To elute DNA, 30 µL of warm DNA Elution buffer was added to the column, left to stand for 1 minute and centrifuged for 15 seconds. All centrifugation steps were performed at 14 500 x g.

B7. DNA restriction digestion protocol

The reagents were set up as follows:

Sterile de-ionised water	16 µl
10X restriction buffer	2 µl
DNA (100-300 ng)	2 µl

The reaction was initiated by adding 1 µL of restriction enzyme and the reaction allowed to proceed for at least 15 minutes at 37˚C or as recommended. To stop the reaction, 4 µl of gel loading buffer (0.25 % bromophenol blue + 30 % glycerol) was added.

Appendix C – Reagents and suppliers

Reagent	Supplier
Acetone	Sigma, U.S.A
Agar bacteriology	Merck, Germany
Agarose	Whitehead Scientific, South Africa
Ammonium persulphate	Merck, Germany
Ampicillin	Roche, Germany
Bradford reagent	Sigma, U.S.A
Bromophenol blue	Sigma, U.S.A
Coomasie brilliant blue R250	Amersham, U.S.A
Chloramphenicol	Roche, Germany
Chloroauric acid	Sigma, U.S.A
DNA ladder	Fermentas, U.S.A
Ethidium bromide	Sigma, U.S.A
Fat free milk	Clover, S.A
Glacial acetic acid	Merck, Germany
Gluteraldehyde	Merck, Germany
Glycerol	Merck, Germany
Glycine	Sigma, U.S.A
HisPur Ni-NTA	Thermoscientifc, U.S.A
Hydrogen peroxide	Merck, Germany
Imidazole	Sigma, U.S.A
Isopropyl-1-thio- β-D-galacopyranoside	Roche, Germany
Lysozyme	Roche, Germany
Methanol	Merck, Germany
Mercaptoethanol	Merck, Germany
Magnesium chloride	Merck, Germany
Malate dehydrogenase	Sigma, USA
Nitrocellulose paper	Thermoscientific, U.S.A
Osmium tetroxide	Merck, Germany
Potassium chloride	Merck, Germany
Potassium dihydrogen phosphate	Merck, Germany
Phenylmethylsufonyl fluoride	Sigma, U.S.A
Polyacrylamide	Sigma, U.S.A
Polyethylene glycol 2 000	Merck, Germany
Polyethylenimine	Sigma, U.S.A
Restriction enzymes	Thermoscientific, U.S.A

Sodium citrate trihydrate	Sigma , U.S.A
Sodium chloride	Merck, Germany
Sodium dodecyl sulphate	Merck, Germany
Sodium hydroxide	Merck, Germany
Snakeskin™ dialysis tubing	Pierce, U.S.A
TEMED	Sigma, U.S.A
Tris	Sigma, U.S.A
Tryptone	Merck, Germany
Tween 20	Merck, Germany
X-ray film	Thermoscientific, U.S.A
Yeast	Merck, Germany

References

Ailon, K., Xie, Y., El-Gendy, N., Berkland, C., & Forrest, M. (2009). Effects of nanomaterial physicochemical properties on in vivo toxicity. *Adv. Drug. Deliv. Rev.* **61**: 457-466.

Akiyoshi, K.S. (1999). Molecular chaperone activity of hydrogel nanoparticles of hydrophobized pullulan: Thermal stabilisation with refolding of carbonic anhydrase B. *Bioconjug.Chem*. 321-324.

Ang, D., Liberek, K., Skowyra, D., Zylicz, M., & Georgopoulos, C. (1991). Biological role and regulation of the universally conserved heat shock proteins. *J. Biol. Chem.* **266**: 24233–24236.

Arora, S., Rajwade, J.M., & Paknikar, K.M. (2012). Nanotoxicology and *in vitro* studies: The need of the hour. *Toxicology and Applied Pharmacology.* **258**: 151-165.

Arvizzo, R.R., Miranda, O.R., Thompson, M.A., Pabelick, C.M., Bhattacharya, R., Roberston, J.D., Rotello, V.M., Prakash, Y.S., & Mukherjee, P. (2010). Effect of nanoparticle surface charge at the plasma membrane and beyond. *Nano. Letters.* **10**: 2543-2548.

Balasubramanian, S.K., Jittiwat, J., Manikanda, J., Ong, C.N., Yu, L.E., & Ong, W.Y. (2010). Biodistribution of gold nanoparticles and gene expression changes in liver and spleen after intravenous administration in rats. *Biomaterials.* **31**: 2034-2042.

Basha, E., Lee, G., Demeler, J. B., & Vierling, E. (2004). Chaperone activity of cytosolic small heat shock proteins from wheat. *Eur. J. Biochem.* **271**: 1426-1436.

Bhattacharya, S., & S. A. (2003). Synthesis of gold nanoparticles stabilised by metal-chelators and the controlled f ormation of close-packed aggregates by them. *Proc. Indian Acad. Sci. Chem. Sci.* **115**: 613-619.

Boshoff, A., Nicoll, W., Hennessy, F., Ludewig, M., Daniel, S., Modisakeng, K., Shonhai, A., McNamara, C., Bradley, G. & Blatch, G.L. (2004). Molecular chaperones in biology, medicine and protein biotechnology. *South African journal of science*. 665-667.

Brayner, R., Ferrari-lliou, R., Brivois, N., Djediat, S., Benedetti, M., & Fievet, F. (2006). Toxicological impact studies based on Escherichia coli bacteria in ultrafine ZnO nanoaprticles colloidal medium. *Nano. Lett.* **6**: 866-870.

Brust, M., Walker, M., Bethell, D., Schifrin, D., & Whyman, R. (1994). Synthesis of thiol derivated gpold naoparticles in a two phase liquid-liquid system. *J. Chem. Soc. Chem. Commun.* **7**: 801-802.

Bukau, B. A., & Horwich, A. (1998). The Hsp70 and Hsp 60 chaperone machines. *Cell.* **92**: 351-366.

Bukau, B., & Walker, G. (1989). Cellular defects caused by deletion of *Escherichia coli* DnaK gene indicate role roles for heat shock protein in normal metabolism. *J. Bacteriol.* **171**: 2337-2346.

Bukau, B., & Walker, G.C. (1990) Mutations altering heat shock specific subunit of RNA polymerase suppress major cellular defects of *E. coli* mutants lacking the DnaK chaperone. *EMBO J*. **9**: 4027-4036

Casadevall, M., da Cruz Fresco. P., & Kortenkamp, A. (1999). Chromium (VI) mediated DNA damage: oxidative pathways resulting in formation of DNA breaks and abasic sites. *Chemico-Biological Interactions.* **123**: 117-132.

Chapell, T., Konforti, B., Schmid, S., & Rothman, J. (1987). The ATPase core of a clathrin uncoating protein. *J. Biol. Chem.* **262**: 746-751.

Chatterjee, T., Chakraborti, S., Joshi, P., Singh, S.P., Gupta, V., & Chakraborti, P. (2010). The effect of zinc oxide nanoparticles on the structure of the periplasmic domain of the *Vibrio cholerae* ToxR protein. *Febs. J.* **277**: 4184–4194.

Chatterjee, S., Bandyopadhyay, A., & Sarkar, K. (2011). Effect of iron oxide and gold nanoparticles on growth leading towards biological application. *Journal of Nanobiotechnology*. **9**: 34.

Chili, M., & Revaprasadu, N. (2008). Synthesis of anisotropic gold nanoparticles in a water soluble polymer. *Materials Letters*. **62**: 3896-3899.

Cho, W.S., Cho, M., Jeong, J., Choi, M., Cho, H.Y., Han, B.S., Kim, S.H., Kim, H.O., Kim, Y.T., Chung, B.H., & Jeong, J. (2009). Acute toxicity and pharmacokinetics of 13 nm sized PEG-coated gold nanoparticles. *Toxicology and Applied Pharmacology.* **236**: 16-24.

Cho, W.S., Cho, M., Jeong, J., Choi, M., Han, B.S., Shin, H.S., Hong, J., Chung, B.H., Jeong, J., & Cho, M.H. (2010). Size-dependent tissue kinetics of PEG-coated gold nanoparticles. *Toxicol. Appl. Pharmacol.* **245**: 116-123.

Connor, E., Mwamuka, J., Gole, A., Murphy, C., & Wyatt, M. (2005). Gold nanoparticles are taken up by human cells but do not cause acute cytotoxicity. *Small.* **1***:* 325-327.

Craig, E., Gambill, B., & Nelson, R. (1993). Heat shock proteins molecular chaperones of protein biogenesis. *Microbiol. Rev.* **57**: 402–414.

Cui, W., Li, J., Zhang, Y., Rong, H., Lu, W., & Jiang, L. (2012). Effects of aggregation and the surface properties of gold nanoparticles on cytotoxicity and cell growth. *Nanomedicine: Nanotechnology, biology and Medicine.* **8**: 46-53.

De Jong, W., & Borm, P. (2008). Drug delivery and nanoparticles: applications and hazards. *Int. J. Nanomedicine.* **311:** 133-149.

De, M., & Rotello, V. (2008). Synthetic "chaperones": nanoparticle mediated refolding of thermally denatured proteins. *Chem. Commun (Camb)*, 3504 - 3506.

Dementо, S.L., Eisenbarth, S.C., Foellmer, H.G., Platt, C., Caplan, M.J., Mark, S.W., Mellman, I., Ledizet, M., Fikrig, E., Flavell, R.A., & Fahmy, T.M. (2009). Inflammasome-activating nanoparticles as modular systems for optimizing vaccine efficacy. *Vaccine.* **23**: 3013-3021.

Doyen, M., Bartik, K., & Bruylants, G. (2013). UV-Vis and NMR study of the formation of gold nanoparticles by citrate reduction. Observation of gold citrate aggregates. *J. of Colloid and Interface Science.* **399**: 1-5.

Dunpall, R., Nejo, A.A., Pullabhotla, V.S.R., Opoku, A,R., Revaprasadu, N., & Shonhai, A. (2012). An *In vitro* assessment of the interaction of Cadmium Selenide Quantum Dots with DNA, Iron, and Blood Platelets. *IUBMB Life.* **64**: 995-1002.

Ellis, J. (1996). Stress proteins as molecular chaperones. In: van Eden, W.; Young, D. (eds) Stress proteins in medicine. Marcel Dekker, New York, 1-26.

Fei, L., & Perret, S. (2009). Effects of nanoparticles on protein folding and fibrillogenesis. *Int. J. Mol. Sci.* **10:** 646-655.

Freese, C., Uboldi, C., Gibson, M.I., Unger, R.E., Weksler, B.B., Romero, I.A., Couraud, P.O., & Kirkpatrick C.J. (2012). Uptake and cytotoxicity of citrate gold nanospheres: comparative studies on human endothelium and epithelial cells. *Particle and Fibre Toxicology.* **9**:23

Fu, G., Vary, P.S., & Lin, C.T. (2005). Anatase TiO2 composites for antimicrobial coatings. *J. Phys. Chem. B.* **109**: 8889-8898.

Gagner, J.E., Qian, X., Lopez, M.M., Dordick, J.S., & Siegel, R.W. (2012). Effect of gold nanoparticle structure on the conformation and function of adsorbed proteins. *Biomaterials*. **33**: 8503-8516.

Georgopoulos, C. (1977). A new bacterial gene(groPC) which affects lambda DNA replication. *Mol. Gen. Genet.* **151**: 35-39.

Georgopoulos, C., Lam, B., Lundquist-Heil, A., Rudolph, C., Yochem, J., & Feiss, M. (1979). Identification of the *E.coli* DnaK (groPC756) gene product. *Mol. Gen. Genet.* **172**: 143-149.

Gething, M., & Sambrook, J. (1992). Protein folding in the cell. *Nature.* **355**: 33-45.

Goodman, C., McCusker, C., Yilmaz, T., & Rotello, V. (2004). Toxicity of gold nanoparticles functionalized with cationic and anionic side chains. *Bioconjug. Chem.* **15**: 897-900.

Govorov, A.O., Zhang, W., Skeini, T., Richardson, H., Lee, J., & Kotov, N.A. (2006). *Nanoscale Res. Lett.* **1**: 84-90.

Gragerov, A., Zeng, L., Zhao, X., Burkholder, W., & Gottesman, M. (1994). Specificity of DnaK-peptide binding. *J. Mol. Biol.* **235**: 848-854.

Hartl, F., Bracher, A., & Hayer-Hartl, M. (2011). Molecular chaperones in protein folding and proteostasis. *Nature.* **475**: 324–332.

Hartl, F., Martin, J., & Neupert, W. (1992). Protein folding in the cellthe role of molecular chaperones Hsp70 and Hsp60. *Annu. Rev. Biophys. Biomol. Struct.* **21**: 293–322.

Hauck, T.S., Ghazani, A.A., & Chan, W.C.W. (2008). Assessing the effect of surface chemistry on gold nanorod uptake, toxicity and gene expression in mammalian cells. *Small.* **4**: 153-159.

Herdt, A.R., Drawz, S.M., Kang, Y., & Taton, T.A. (2006). DNA dissociation and degradation at gold nanoparticle surfaces. *Colloids and Surfaces B: Biointerfaces.* **51**:130-139.

Hermanson, G.T. (1996). Bioconjugate Techniques. *Academic Press,* San Diego.

Horie, M., Nishio, K., Fujita, K., Endoh, S., Miyauchi, A., Saito, Y., Iwahashi, H., Yamamoto, K., Murayama, H., Nakano, H., Nanashima, N., and Niki, E. et al (2009). Protein adsoprtion of ultrafine metal oxides and its influence on cytotoxicity toward culture cells. *Chem. Res. Toxicol.* **22**: 543-553.

Hoyt, V.W., & Mason, E. (2008). Nanotechnology emerging health issues. *J. Chem. Health. Sci.* **15**: 10-15.

Huang, X.H., Jain, P.K., El-Sayed, I.H., & El-Sayed, M.A. (2007). *Nanomedicine.* **2**: 681-693.

Hung, L., & Leel, A. (2007). Microfluidic devices for the synthesis of nanoparticles and biomaterials. *J. Med. Biol. Eng.* **27**: 1-6.

Jia, H., Liu, Y., Zhang, X.J., Han, L., Du, L.D., Tian, Q & Xu, Y.C. (2009). Potential oxidative stress of gold nanoparticles by induced-NO releasing in serum. *J. Am. Chem. Soc.* **131**: 40-41.

Khlebstov, N., Dykman, L. (2010). Biodistribution and toxicity of engineered gold nanoparticles: a review of *in vitro* and in vivo studies. *Chem. Soc. Rev.* **40**: 1647-1671.

Klein J. (2007). Probing the interactions of proteins and nanoparticles. *Proc. Natl. Acad. Sci.* USA. **104**: 2029-30.

Kogan, M.J., Bastus, N.G., Amigo, R., Grillo-Bosch, D., Arraya, E., Turiel, A., Labarta, A., Giralt, E., & Puntes, V.F. (2006). *Nano Lett.* **6**: 110-115.

Koser, S. (1924). Correlation of citrate utilisation by members of the colon-aerogenes group with other differential characteristics and with habitat. *J. Bacteriol.* **9**: 59

Kumar, S., Harrison, N., Richards-Kortum, R., & Sokolov, K. (2007). *Nano Lett*. **7**: 1338-1343.

Lewinski, N., Colvin, V., & Drezek, R. (2008). Cytotoxicity of nanoparticles. *Small.* **4**: 26-49.

Li, N., Ma, L., Wang, J., Zheng, L., Liu, J., Duan, Y., Liu, H., Zhao, X., Wang, S., Wang, H., Hong, F., & Xie, Y. (2010). Interaction between Nano-Anatase TiO2 and Liver DNA from Mice In Vivo. *Nanoscale Res. Lett*. **5**: 108-115.

Lindquist, S., & Graig, E. (1988). The heat shock proteins. *Annu. Rev. Genet.* **22**: 631-677.

Liu, J., & Vipulanandan, C. (2013). Effects of Au/Fe and Fe nanparticles on *Serratia* bacterial growth and production of biosurfactant. *Materials Science and Engineering C.* **33**: 3909-3918.

Love, J.C., Estroff, L.A., Kriebel, J.K., Nuzzo, R.G., & Whitesides, G.M. (2005). Self-assembled monolayers of thiolates on metals as a form of nanotectnology. *Chem. Rev.* **105**: 1103-1169.

Luthuli, S.D., Chili, M.M., Revaprasadu, N., & Shonhai, A. (2013). Cysteine-capped gold nanoparticles suppress aggregation of proteins exposed to heat stress. *IUBMB Life*. **65**: 454-461.

Lynch, I., Cedervall, T., Lundqvist, M., Cabaleiro-Lago, C., Linse, S., & Dawson, K. (2007). The nanoparticle–protein complex as a biological entity; a complex fluids and surface science challenge for the 21st century. *Adv. Colloid Interface Sci*. 167–174.

Mandal, S., Selvakannam, P., Phadtare, S., Passicha, R., & Sastry, M. (2002). Synthesis of a stable gold hydrosol by the reduction of chloroaurate ions by the amino acid aspartic acid. *Pro. Indian Acad. Sci. Chem. Sci.* **114**: 513-520.

Mayer, M. (2010). Gymnastics of molecular chaperones. *Mol. Cell.* **39**:321–331.

Mayer, M.P., Rüdinger, S., and Bukau, B. (2000). Molecular basis for interactions of the DnaK chaperone with substrates. *Biol. Chem.* **381**: 877–885.

Mayer, M., Schröder, H., Rüdinger, S., Paal, K., Laufen, T., & Bukau, B. (2000). Multistep mechanism of substrate binding determines chaperone activity of Hsp70. *Nat. Struct. Biol.* **7**: 586-593.

McQuillan, J. (2010). Bacterial-Nanoparticle Interactions. PhD Thesis. University of Exeter.

Mogk, A., Bukau, B., Lutz, R., & Schumann, W. (1999). Construction of hybrid *Escherichia coli-Bacillus subtilis* DnaK genes. *J. Bacteriol.* **181**: 1320-1328.

Montgomery, D., Jordan, R., McMacken, R., & Freire, E. (1993). Thermodynamic and structural analysis of the folding/unfolding transitions of the *Escherichia coli* molecular chaperone DnaK. *J. Mol. Biol.* **232**: 680–692.

Morimoto, R., Tissieres, A., & Georgopoulos, C. (1994). Progress and perspectives on biology of heat shock proteins and molecular chaperones. In: Morimoto, R.I., Tissieres, A., Georgopoulos,

C. (ad) *The biology of heat shock proteins and molecular chaperones*. New York, Cold Spring Harbour laboratory Press. (1994): 1-30.

Nel, A., Xia, T., Madler, L., & Li, N. (2006). Toxic potential of materials at the nanolevel. *Science.* **311**: 622 – 627.

Nghiem, T.H.L., La, T.H., Vu, T.H., Chu, V.H., Nguyen, T.H., Le, Q.H., Fort, E., Do, Q.H., & Tran, H.N. (2010). Synthesis, capping and binding of colloidal gold nanoparticles to proteins. *Adv. Nat. Sci: Nanosci. Nanotechnol.* **1**: 025009 (5pp).

Nguyen, T.D., Kim, D.J., So, M.G., & Kim, K.S. (2010). Experimental measurements of gold nanoparticle nucleation and growth by citrate reduction of $HAuCl_4$. *Adv. Powder. Tech.* **21**: 111-118.

Paek, K., & Walker, G. (1987). Escherichia coli DnaK null mutants are inviable at high temperature. *J. Bacteriol.* **169**: 283-290.

Pak, M., and Wickner, S. (1997) Mechanism of protein remodelling by ClpA chaperone. *Proc. Natl. Acad. Sci.* U.S.A. **94**: 4901–4906

Pan, Y., Leifert, A., Ruau, D., Neuss, S., Bornemann. J., Schmid, G., Brandau, W., Simon, U., & Jahnen-Dechent, W. (2009). Gold nanoparticles of diameter 1.4nm trigger necrosis by oxidative stress and mitochondrial damage. *Small.* **5**: 2067-2076.2

Patil, S., Sandberg, A., Heckert, E., Self, W., and Seal, S (2007). Protein adsorption and cellular uptake of cerium oxide nanoaprticles as function of zeta potentail . *Biomaterials.* **28**: 4600-4607.

Patra, H.K., Banerjee, S., Chaudhuri, U., Lahiri, P., Dasgupta, A.K. (2007). *Nanomed: Nanotechnol. Biol. Med.* **3**: 111-119.

Perez-Juste, J., Pastoriza-Santos, I., Liz-Marzem, L., & Mulvaney, P. (2005). *Coord. Chem. Rev.* **249** :1870 - 1901.

Pooja, M., V. Komal, V., Vida, A., & Shree, R. (2011). Functionalized Gold nanoparticles and their biomedical applications. *Nanomaterials.* **1**: 31 -63.

Priester, J., Stoimenov, P., Mielke, R., Webb, S., Ehrhardt, C., Zhang J., Stucky, G., & Holden, P. (2009). Effects of soluble cadmium salts versus CdSe quantum dots on the growth of planktonic *Pseudomonas aureginosa*. *Environ. Sci. Technol.* **43**: 2589-2594

Rana, S., Bajaj, A., Mout, R., & Rotello, V.M. (2012). Monolayer coated gold nanoparticles for delivery applications. *Advanced Drug delivery reviews.* **64**: 200-216.

Ready, V. (2006). Gold nanoparticles: Synthesis and applications. 1791.

Shipway, A.N., Katz, E., & Wilner, I. (2000). Nanoparticle arrays on surfaces for electronic, optical and sensor applications. *Chem. Phys. Chem.* **1**: 18-52.

Shonhai, A., Boshoff, A., & Blatch, G.L. (2005). Plasmodium falciparum heat shock protein 70 is able to suppress the thermosensitivity of an *Escherichia coli* DnaK mutant strain. *Mol Genet Genomics*. **274**: 70–78.

Shonhai, A., Botha, M., Beer. T.A.P., Boshoff, A., and Blatch, G.L. (2008). Structure-function analysis of *Plasmodium falciparum* heat shock protein 70 using three dimensional modelling and *in vitro* analysis. *Protein Pept. Lett.* **15**: 1117-1125.

Shröder, H., Langer, T., Hartl, F-U. & Bukau, B. (1993). DnaK, DnaJ, Grp E form a cellular chaperone machinery capable of repairing heat induced protein damage. *EMBO. J.* **12**: 4137-4144.

Sinha, R., Karan, R., Sinha, A., & Khare, S. (2010). Interaction and nanotoxic effect of ZnO and Ag nanoparticles on mesophilic and halophilic bacterial cells.*Bioresource technology*. **102**: 1516-20.

Sivaranam, S.K., Kumar, S., & Santhanam, V. (2011). Mono-disperse sub-10 nm gold nanoparticles by reversing the order of addition in Turkevich method. The role of chloroauric acid. *Journal of colloid and Interface Science.* **361**: 543-547.

Skerman, V. (1960). A guide to the identification of the genera of bacteria. *Acad. Med.* **35**: 92

Sobczak-Kupiec, A., Malina, D., Zimowska, M., & Wzorek, Z. (2011). Characterisation of gold nanoparticles for various applications. *Digest Journal of Nanomaterials and Biostructures.* **6**: 800-808.

Sonnichsen, C., & Alivisatos, P. (2005). Gold nanorods as novel non bleaching plasmon-based orientation sensors for polarized single-particle microscopy. *Nano Lett.* **5**: 301 - 305.

Spence, J., Cegielska, A., & Georgopoulos, C. (1990). Role of *Escherichia coli* heat shock proteins DnaK and HtpG (C62.5) in response to nutritional deprivation. *J. Bacteriol.* **172**: 7157-7166.

Sperling, R.A, Gil, P., Zhang, F., Zanella, M., & Parak, W.J. (2008). Biological applications of gold nanoparticle. *Chem. Soc.Rev*. **37**: 1896-1908.

Sperling, R.A., Pellegrino, I., Li, J.K., Chang, W.H., & Parak, W.J. (2006). *Adv. Funct. Matter.* **16:** 943-948.

Stirling, P. C., Lundin, V. F., and Leroux, M. R. (2003) Getting a grip on non-native proteins. EMBO Rep. 4: 565-570.

Tabrizi, A., Ayhan, F., & Ayhan H. (2009). Gold nanoparticle synthesis and characterisation. *HACETTEPE Journao of Biology and Chemistry.* 37: 217-226.

Theis, T. (2001). Nanotechnology: A revolution in the making. *Nanotech Defined,* IBM Research

Tilly, K., McKittrick, N., Zylicz, M., & Georgopoulos, C. (1983). The DnaK protein modulates the heat shock response of *Escherichia coli*. *Cell.* **34**: 641-646.

Turkevich, J., Stevenson, P., & Hillier, J. (1951). A study of nucleation and growth process in the synthesis of colloidal gold. *Faraday. Soc.* **11**:55-75.

Uboldi, C., Bonachi, D., Lorenzi, G., Hermans, M.I., Pohl, C., Baldi, G., Unger, R.E., & Kirkpatrick, C.J. (2009). Gold nanoparticles induce cytotoxicity in the alveolar type II cell lines A549 and NCIH 441. *Port. Fibre. Toxicol.* **6**: 18.

Unfried, K., Uzun, O., Klotz, L., Von Mickecz, A., Grether-Beck, S., & Schins, R. (2007). Cellular responses to nanoparticles: target structures and mechanisms. *Nanotechnology* **1**: 52-71.

van Montfort, R. L. M., Basha, E., Friedrich, K. L., Slingsby, C. and Vierling, E. (2001) Crystal structure and assembly of a eukaryotic small heat shock protein. *Nature Struct. Biol.* **8**: 1025–1030.

Veinger, I., Diamant, S., Buchner, J., & Goloubinoff, P. (1998). The small heat shock protein IbpB from *Escherichia coli* stabilises stress denatured proteins for subsequent refolding by a multi-chaperone network. *J. Biol. Chem.* **273**: 11032-11037.

Verma, A., & Rotello, V. (2005). Surface Recognition of Biomacromolecules Using Nanoparticle Receptor. *Cheminform.* **36**: no. doi: 10.1002/chin.200519285.

Vertegel, A., Siegel, R., & Dordick, J. (2004). Silica nanoparticle size influences the structure and enzymatic activity of adsorbed lysozyme. *Langmuir.* **20**: 6800-6807.

Walter, S. (2002). Structure and function of the Group E chaperone. *Cell Mol. Life Sci.***59**: 1589 - 1597.

Wang, L., Sun, N., Terzyan, S., Zhang, X., & Benson, D. (2006). *Biochemistry.* **45**: 13750-13759.

Yang, J., Pong, B-K., Lee, J.Y., & Too, H-P. (2007). Dissociation of double stranded DNA by small metal nanoparticles. *Journal of Inorganic Biochem.* **101**: 824-830.

Young, J., Agashe, V., Siegers, K., & Hartl, F. (2004). Pathways of chaperone-mediated protein folding in the cytosol. *Nat. Rev. Mol. Cell Biol.* **5**: 781-791.

Zaqout, M.S.K., Sumizawa, T., Igisu, H., Wilson, D., Myojo, T., and Ueno, S. (2012). Binding of titanium dioxide nanopartilces to lactate dehydrogenase. *Environ. Health. Prev. Med.* **17**: 341-345.

Zhang, D., Neumann, O., Wang, H., Yuwono, V.M., Barhoumi, A., Perham, M., Hartegerink, J.D., Wittung-Stafshede, P., and Halas, N.J. (2009). Gold nanoparticles can induce the formation of Protein-based aggregates at Physiological pH. *Nano Lett*. **9**: 666-671.

Zhao, L., Jiang, D., Cai, Y., Ji, X., Xie, R., & Yang, W. (2012). Tuning the size of gold nanoparticles in the citrate reduction by chloride ions. *Nanoscale.* **4**: 5071-5076.

Zhou, Y., Kong, Y., Kundu, S., Cirillo, J.D., & Liang, H. (2012). Antibacterial activities of gold and silver nanoparticles against *E.coli* and *bacillus* Calmete-Guerin. *J. of Nanobiotech.* **10**: 19.